The Astronomical Journal, 156:275 (23pp), 2018 December https://doi.org/10.3847/1538-3881/aae9ec

The Rotational Evolution of Young, Binary M Dwarfs

John Stauffer[1], Luisa M. Rebull[1,2], Ann Marie Cody[3], Lynne A. Hillenbrand[4], Marc Pinsonneault[5], David Barrado[6], Jerome Bouvier[7], and Trevor David[8]
[1] Spitzer Science Center (SSC), IPAC, California Institute of Technology, Pasadena, CA 91125, USA; stauffer@ipac.caltech.edu
[2] Infrared Science Archive (IRSA), IPAC, California Institute of Technology, 1200 E. California Blvd, MS 100-22, Pasadena, CA 91125, USA
[3] NASA Ames Research Center, Space Sciences and Astrobiology Division, MS245-3, Moffett Field, CA 94035, USA
[4] Astronomy Department, California Institute of Technology, Pasadena, CA 91125, USA
[5] Astronomy Department, The Ohio State University, Columbus, OH 43210, USA
[6] Centro de Astrobiología, Dpto. de Astrofísica, INTA-CSIC, E-28692, ESAC Campus, Villanueva de la Cañada, Madrid, Spain
[7] Univ. Grenoble Alpes, IPAG, F-38000, Grenoble, France
[8] Jet Propulsion Laboratory, California Institute of Technology, M/S 321-100, 4800 Oak Grove Drive, Pasadena, CA 91109, USA
Received 2018 May 25; revised 2018 October 15; accepted 2018 October 16; published 2018 November 21

Abstract

We have analyzed *K2* light curves for more than 3000 low-mass stars in the ∼8 Myr old Upper Sco association, the ∼125 Myr age Pleiades open cluster, and the ∼700 Myr old Hyades and Praesepe open clusters to determine stellar rotation rates. Many of these *K2* targets show two distinct periods, and for the lowest-mass stars in these clusters, virtually all of these systems with two periods are photometric binaries. The most likely explanation is that we are detecting the rotation periods for both components of these binaries. We explore the evolution of the rotation rate in both components of photometric binaries relative to one another and to nonphotometric binary stars. In Upper Sco and the Pleiades, these low-mass binary stars have periods that are much shorter on average and much closer to each other than would be true if drawn at random from the M dwarf single stars. In Upper Sco, this difference correlates strongly with the presence or absence of infrared excesses due to primordial circumstellar disks—the single-star population includes many stars with disks, and their rotation periods are distinctively longer on average than their binary star cousins of the same mass. By Praesepe age, the significance of the difference in rotation rate between the single and binary low-mass M dwarf stars is much less, suggesting that angular momentum loss from winds for fully convective zero-age main-sequence stars erases memory of the rotation rate dichotomy for binary and single very low mass stars at later ages.

Key words: binaries: general – stars: low mass – stars: pre-main sequence – stars: rotation

Supporting material: machine-readable tables

1. Introduction

There have been a number of observational programs aimed at determining the initial distribution of rotation rates for low-mass stars (e.g., Bouvier et al. 1986; Hartmann et al. 1986; Herbst et al. 2001; Rebull et al. 2002; Affer et al. 2013; Moraux et al. 2013). Quite a few observational papers have also been devoted to determining the multiplicity function for low-mass stars, both in young populations (e.g., Ghez et al. 1993; Bouvier et al. 1997; Kraus et al. 2008; Shan et al. 2017) and among field stars of indeterminate age (e.g., Duquennoy & Mayor 1991; Fischer & Marcy 1992; Reid & Gizis 1997; Janson et al. 2012). However, it has seldom if ever been possible to conduct sensitive surveys with large sample sizes that simultaneously place strong constraints on both rotation rates and multiplicity. If such a survey could be conducted, it could potentially provide valuable new insights into how binary (and single) stars are formed and evolve.

In fact, a facility that could simultaneously identify binary stars and measure rotation rates for large populations of young, low-mass stars in nearby open clusters and star-forming regions did become available in 2014. That facility is NASA's *K2* space telescope (Howell et al. 2014). *K2* has now provided high-precision, rapid-cadence, long-duration, sensitive light curves for a large fraction of the members in several of the nearest and best-studied nearby star-forming regions and open clusters. Those light curves not only allow determination of the rotation periods for a very large percentage of the target stars, but they also provide rotation periods for both components of many of the binary systems (i.e., where there is enough light from the secondary to detect its rotational modulation as well as that of the primary star). Because the ages for these clusters are well determined, it should be possible to use these data to place new empirical constraints on the evolution of rotation and multiplicity with time.

In this paper, we use our *K2* rotational periods for the Upper Sco association (age ∼8 Myr), the Pleiades (age ∼125 Myr), and the older (age ∼700 Myr) Hyades and Praesepe open clusters to highlight possible evidence that the rotation rates and multiplicity of low-mass stars are strongly linked at 8 Myr, with stars in photometric binary systems being both more rapidly rotating and with the two components of the binaries having rotation rates closer to each other than would be true if drawn randomly from the single-star population. In Section 2, we describe the sources of data for this paper. In Section 3, we document the ability of *K2* to determine the rotation periods for both component stars of binary M dwarf stars (dMs). In Section 4, we compare the rotation rates of the single and binary $M < 0.32\,M_{\odot}$ M dwarfs in Upper Sco, Pleiades, Hyades, and Praesepe, and we provide evidence that the binary and single stars have different rotational velocity distributions at young ages. In Section 5, we describe a Monte Carlo simulation which supports our conclusion that the binary dMs in Upper Sco and the Pleiades are faster rotating and have more closely paired rotation rates than would be true if drawn from the single dM population. Finally, in Section 6, we discuss

links of these differences to the presence of pre-main-sequence (PMS) disks, and in Section 7 we discuss some of the properties of the binary populations in Upper Sco and the Pleiades and how those properties help us interpret the rotation period data.

2. Observational Data

All of the rotation period data we use in this paper come from light curves obtained by NASA's *K2* mission. We use the periods we have previously derived and reported in Rebull et al. (2016a, 2016b) for the Pleiades, Rebull et al. (2017) for Praesepe, Rebull et al. (2018) for Upper Sco, and to be reported in an upcoming paper for the Hyades (L. Rebull et al. 2018, in preparation). In those same papers, we provide $(V-K_s)_0$ colors for all of the stars with periods. Where possible, we use observed V and K_s photometry to yield the $(V-K_s)_0$ color; where that was not possible (primarily when there is no literature V magnitude; K_s comes from 2MASS), we use photometry at other bands to allow us to estimate the star's $(V-K_s)_0$ color. Additionally, there is effectively no reddening toward Pleiades, Hyades, or Praesepe; reddening matters for Upper Sco, and our method of dereddening is discussed in Rebull et al. (2018). The set of stars observed by *K2* that we consider to be members of the four clusters is also described in those papers. In general, the membership status is quite good in the Pleiades, Hyades, and Praesepe, and we expect there are relatively few nonmembers in our *K2* cluster catalogs. The situation is considerably worse in Upper Sco, where perhaps 5%–10% of the 1133 stars in our catalog may be nonmembers (Rebull et al. 2018), in addition to the scatter in color introduced by reddening.

Because we believe the Hyades and Praesepe have very similar ages, and because we have comparatively few very low mass stars with *K2* periods in these two clusters, we combine the period data we have for them in all of the plots for this paper.

Upper Sco is young enough that some of its members retain their primordial circumstellar disks, and in many cases those stars are still actively accreting gas. Rebull et al. (2018) identified Upper Sco members with primordial disks by analyzing the spectral energy distributions (SEDs) of those stars; infrared (IR) excesses were identified primarily using 2MASS (Skrutskie et al. 2006), *Wide-field Infrared Survey Explorer* (Wright et al. 2010), and Spitzer (Werner et al. 2004) data. We use the sorting of Upper Sco stars into disk-bearing and nondisk samples in Section 6 of this paper.

3. Setting the Stage: Defining Our M Dwarf Binary Star Sample

Our goal in this paper is to use the *K2* rotation data to determine if there is a correlation between binarity and rotation for low-mass M dwarfs that originates at birth, and whether that correlation—if it exists—persists through the first gigayear on the main sequence. It is possible to use knowledge of the observed properties of low-mass binary systems (Duchene & Kraus 2013) and standard angular momentum evolution models (e.g., Gallet & Bouvier 2015) to predict what we might see. M dwarf binaries, and particularly low-mass M dwarf binaries, are weighted toward relatively small separations (at $<$50 au) and high-q systems (Bergfors et al. 2010; Janson et al. 2012) relative to their higher mass counterparts. For Upper Sco, high-q, small-separation binaries are likely weighted toward systems without inner primordial disks (weak-lined T Tauris, or WTTs) due to the deleterious effects of binarity on disk lifetime and mass (Harris et al. 2012; Kraus et al. 2016). In the standard disk-locking paradigm (Königl 1991), slow rotation is associated with long disk lifetimes; in the absence of disks, PMS stars should spin up from angular momentum conservation. The components of these close binaries should therefore be relatively rapidly rotating at young ages. The fact that the angular momentum loss rate from winds is higher for rapid rotators than slow rotators should eventually eliminate an overall dichotomy in rotation rate between binary stars and single stars. However, because rapidly rotating dM stars should be in the saturated regime where angular momentum loss rates are nearly independent of rotation rate, if both members of a binary are rapid rotators, their rotation rates could initially diverge from each other. Remarkably, these predictions are confirmed by our *K2* data.

Before we can conduct this study, we need to establish three things:

1. That our *K2* data are capable of identifying a reliable binary star population;
2. That there is indeed a built-in preference for rapid rotation among binary stars at very young ages;
3. And that we can determine an appropriate mass range over which to compare dM rotation rates for stars ranging in age from $\sim$10 Myr to $\sim$1 Gyr.

We address each of these points individually in the following sections.

3.1. Using K2 Light Curves to Identify Low-mass Binary Stars

In our *K2* rotation papers, we have identified photometric periods for $>$3000 stars in our four clusters (Upper Sco, Pleiades, Hyades, and Praesepe). Unlike the case for nearly all ground-based efforts, the completeness for detecting rotation periods for the low-mass stars in these clusters is very high ($\gtrsim$90%); therefore, any incompleteness correction for pole-on stars or very slowly rotating stars should have negligible impact on our conclusions.[9] For most of our target stars, there is only one real period identified in the Lomb–Scargle (LS) periodogram. However, the *K2* light curves are so sensitive and have such good cadence and such long durations that we are often able to detect more than one period for a given star when such multiple periods are present. For stars with mass $>1\,M_\odot$, multiple periods normally arise from pulsation (Zwintz et al. 2014; White et al. 2017). For $0.5 < M < 1.0\,M_\odot$, multiple periods or complex/structured peaks in the periodogram are most often due to latitudinal differential rotation and spots at different latitudes or spot evolution (Aigrain et al. 2015; Rebull et al. 2016a, 2016b; Santos et al. 2017); some stars with two LS peaks in this mass range are instead binaries, with each period corresponding to the rotation period of one of the stars in the system. The latter option becomes the more likely scenario when the difference between the two periods is greater than about 20% (i.e., larger than could be explained for a plausible

[9] This completeness estimate is simply the ratio of the number of candidate low-mass members with a *K2* period to the total number of candidate members in our input *K2* cluster sample. Some of the stars with no period could be older field stars mistakenly identified as cluster members. The completeness estimate also does not take binary stars into consideration; that topic is discussed in detail in Appendix C.

degree of latitudinal differential rotation). For $M < 0.5\,M_{\odot}$, particularly for fully convective M dwarfs, both observations and theory suggest that there should be little or no latitudinal differential rotation (Kuker & Rudiger 1997; Browning 2008; Morin et al. 2010; Reinhold et al. 2013; Rappaport et al. 2014). That, combined with the rapid rotation of young dM stars, suggests that, in this mass regime, detection of two periods separated by more than a few percent (Rappaport et al. 2014) likely signals that the star is a binary.[10] Figure 1 shows the *K2* light curves of four dM *K2* binary members of the Pleiades, their LS periodograms, and the phased light curves of both component stars. Here and throughout the rest of the paper, we use the short-hand of "*K2* binary" to mean a low-mass star whose *K2* light curve shows two peaks in its LS periodogram, which we interpret to mean that it is a binary star and that each peak is the rotation period for one component of the binary. We use the term "single" for stars with only one period, but they could be binaries with low-q or tidally locked systems. The phased light curves of all eight of these stars have shapes that are typical of what is seen for the single dM members of the cluster.

Strong confirmation that the dM stars in young clusters with two *K2* periods are best interpreted as high-q binaries is provided in Figure 2, where we show color–magnitude diagrams (CMDs) for our *K2* stars for the Pleiades and Praesepe. The *K2* dM binary stars are nearly always well displaced above the single-star locus in these two diagrams, with a mean $\Delta V > 0.5$ mag. Similar CMDs are not as well defined for Upper Sco because the uncertainty in dereddened color is fairly large, but a clear net displacement between the dM stars with one period and those with two periods is evident (see Figure 13 of Rebull et al. 2018).

3.2. Rotation of M Dwarfs in Upper Sco: Rapid Rotation in Binary dMs Is Built In from Early in PMS Evolution

In Stauffer et al. (2016), we compared the periods for mid-dM (∼M4 to ∼M6) Pleiades stars identified as binaries by *K2* to the periods for the Pleiades *K2* single mid-dM stars. We found that the components of the binary dM systems rotated faster on average, and had periods that were closer to each other, than would have been expected if those periods were drawn at random from the Pleiades single dM population. A Kolmogorov–Smirnov (KS) test and Monte Carlo simulations showed that those differences were significant at better than one in 1000 odds. Other papers reporting evidence that binary, low-mass zero-age main-sequence (ZAMS) stars rotate faster than singles of the same mass include Meibom et al. (2007) and Douglas et al. (2016, 2017).

As touched upon in Rebull et al. (2018) and discussed more thoroughly here, we have now found that for the entire dM color range where we have good sampling (corresponding approximately to spectral types M0–M5.5), the dM *K2* binary stars in the ∼8 Myr Upper Sco association are also faster rotating and have rotation periods closer to each other than if drawn from the single-star population, with an even greater level of significance than in the Pleiades. For this color range ($4.0 < (V-K_s)_0 < 6.5$), we find 147 binary systems and 562 single stars in Upper Sco with periods in our *K2* sample. Figure 3 shows a histogram of the periods for the components of the binary dM systems compared to the single stars; the binary star members are clearly more rapidly rotating. A KS test shows that the probability that the binary and single star rotation periods are drawn from the same parent population is less than one part in 100,000. As another way to highlight the rapid rotation of the dM binary stars, we note that among the 856 ($562 + 2 \times 147$) stars with periods in Figure 3, 34% are members of binaries; however, among the stars with $P <$ 1 day, 57% are members of binaries identified with *K2* (i.e., with two rotation periods).

To illustrate the fact that the two components of the binary systems have periods that are, on average, closer than expected to each other, Figure 4 provides a period–color plot where we separately show (but link) the two components of the 50 binary systems with the shortest primary-star periods and compare these systems to the Upper Sco single dMs. We plot only these most rapidly rotating binary systems for clarity; plotting the entire set of binaries results in so many points in the diagram as to make it difficult for the eye to pick out trends. While the rapid rotation of the primary stars in this plot is, in part, a selection effect, the fact that the period of the secondary differs from that of the primary by an amount so much less than the scatter in period at a given color for the single stars is not a selection effect. In Sections 4 and 5, we provide more quantitative means of assessing the significance of the difference between the binary and single star rotation properties for late dM stars in our four clusters.

3.3. Assigning Masses and Adopting a Common Mass Range

For the remainder of the paper, instead of sorting the stars by their $(V-K_s)_0$ color, we will use their inferred stellar mass. We do this because the mass range for a given $(V-K_s)_0$ range in Upper Sco is very different than the mass range for that same color range in Praesepe/Hyades or the Pleiades. While assigning masses for dM stars on or very near the MS should be relatively uncontroversial, doing so at the age of Upper Sco is still a quite debatable process. In order to allow others to retrace our steps, we describe in the appendix our process for assigning masses to the stars for which we have *K2* light curves.

In order to compare the rotational data in the four clusters, we must choose a common mass range. As we noted previously, angular momentum losses from winds eventually eliminate any initial spread in rotation at a given mass and age (Skumanich 1972; Radick et al. 1987; Pinsonneault et al. 1990). This is seen dramatically in the *K2* data for Praesepe (Rebull et al. 2017), where the great majority of the FGK and early M dwarfs have a well-defined, monotonically decreasing rotation rate with decreasing mass. Any initial spread in rotation rate at a given mass in that spectral type range has been almost completely erased by ∼700 Myr. We therefore choose to set the upper mass limit for our study at the point in mass where the Praesepe slow sequence ends, which is at about $0.32\,M_{\odot}$. This upper mass limit also places us in the mass regime where it is safe to assume that two peaks in the LS periodogram identify the star as a binary (see Figure 2). For the lower mass limit, we choose $0.1\,M_{\odot}$ because it corresponds approximately to the faint limit where we have reasonably good sensitivity and are able to determine periods in most of the stars with *K2* data.

[10] Stars whose phased light curves have significantly nonsinusoidal shapes can also have multiple apparent peaks in their LS periodogram whose periods are harmonics of the rotation period. It is normally easy to determine that these additional peaks are aliases rather than true rotation periods from close examination of the light curve shape and of the periods themselves.

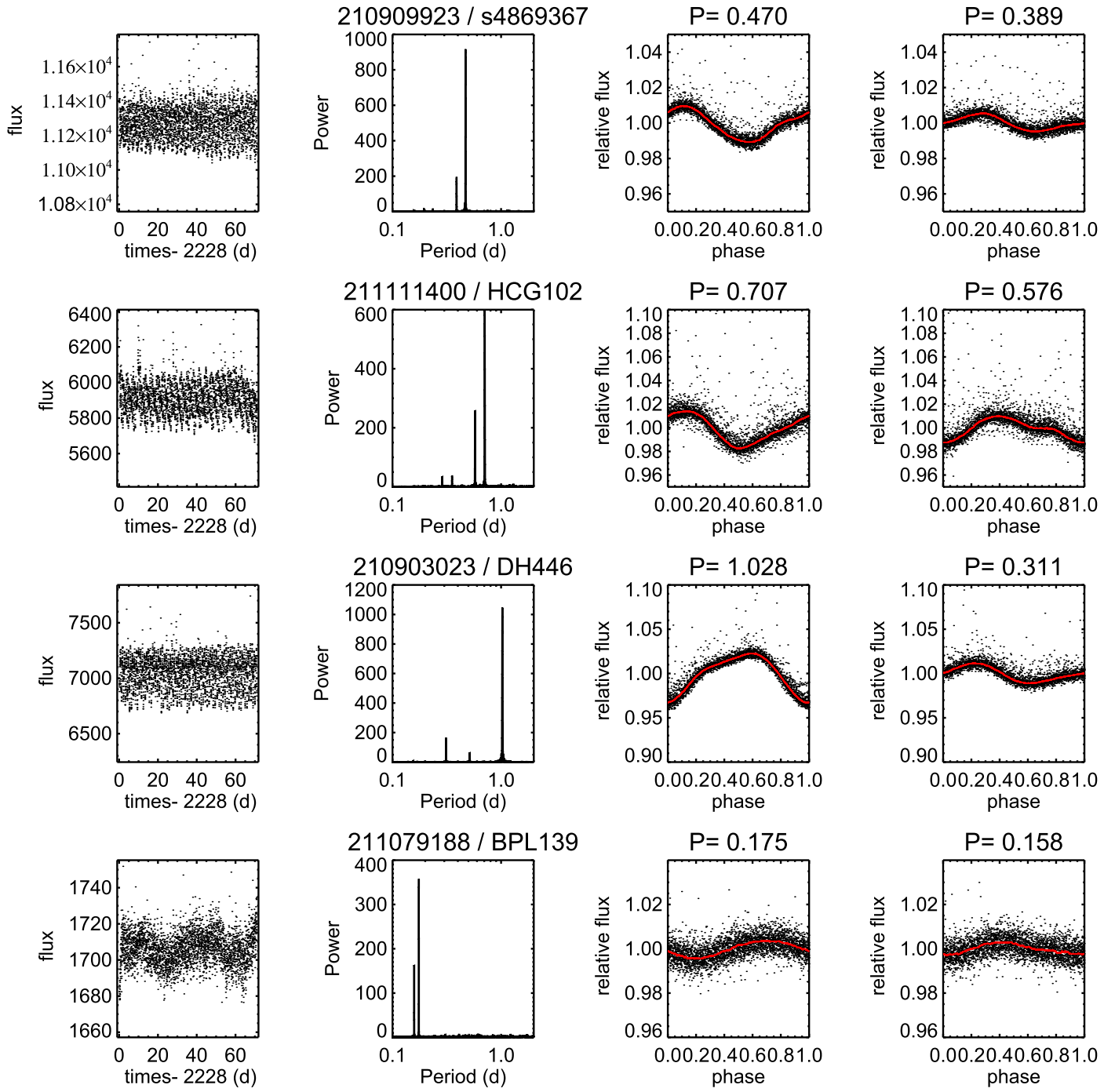

Figure 1. Example light curves (left), LS periodograms (center), and phased light curves (right) for the individual components of four Pleiades dM stars (one per line) with two identified rotation periods. Note that while we can accurately extract the phased light curve shape and amplitude in counts for each component of these binaries, the amount in which each component contributes to the total light of the binary is unknown. For the phased light curves shown here, we have simply divided the observed count rate by the median.

With those choices and with the other demonstrations in the preceding sections, we are now set to proceed to compare the rotation rates of the binary and single stars in our four clusters.

4. Correlation between Rotation and Binarity for Fully Convective, Low-mass Stars at Early Ages

Using the mass calibrations we describe in the appendix, adopting a mass range of $0.1 < M/M_{\odot} < 0.32$, we have a total sample of 257 stars (191 with one *K2* period and 66 with two periods) in Upper Sco, 286 stars in the Pleiades (236 with one period, 50 with two) and 292 stars in Praesepe/Hyades (245 with one period, 47 with two). Tables listing these stars and their $(V-K_s)_0$ colors, rotation periods, and masses are provided in the appendix. Figures 5–7 show mass–period diagrams for the four clusters. Each *K2* binary appears twice in these figures, with the component having the stronger periodogram peak in blue and the star with the weaker periodogram peak in red; stars with just one *K2* period are shown as black dots. While perhaps not "obvious," careful visual inspection of these figures suggests that in this mass range, the binary stars

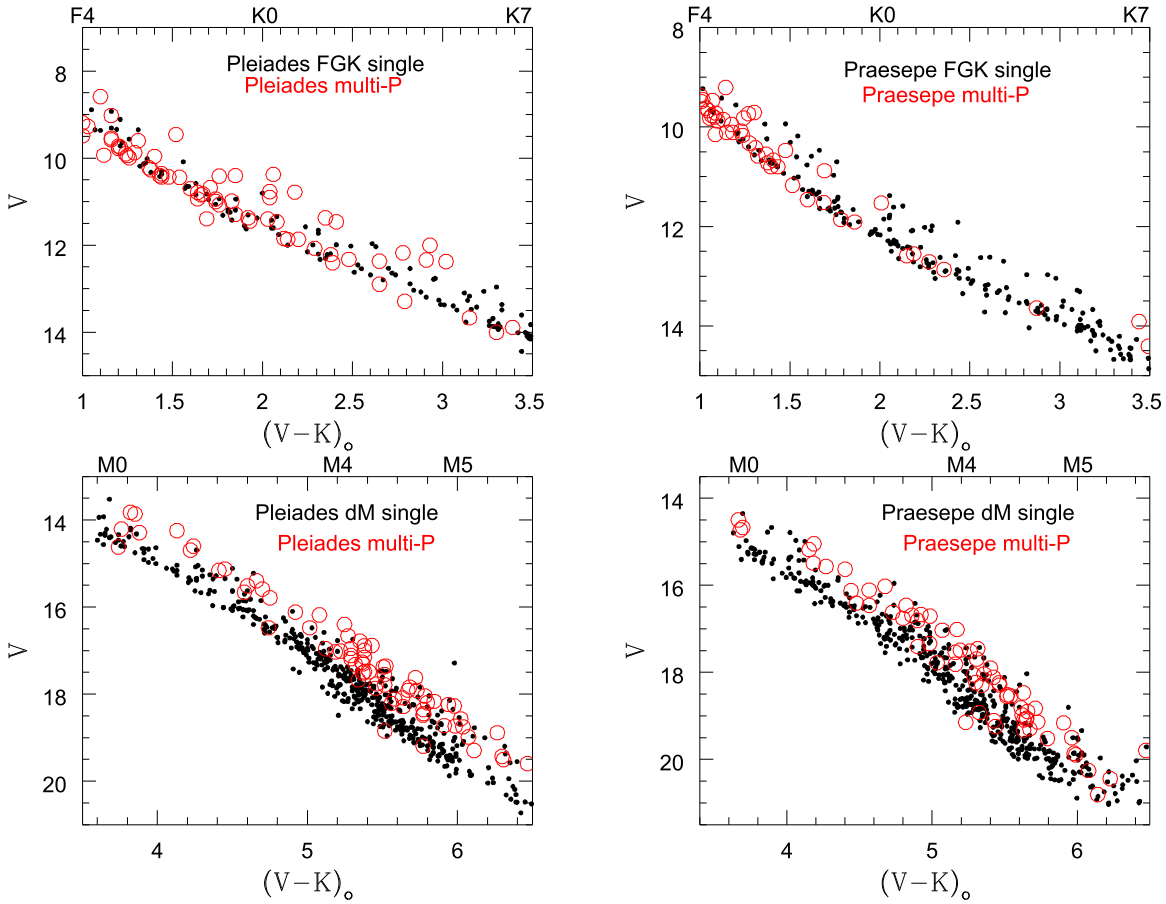

Figure 2. CMDs for two mass ranges in the Pleiades (left) and Praesepe (right). The top row has stars with $M > 0.5\,M_{\odot}$; the bottom row has stars with $M < 0.5\,M_{\odot}$. In all four panels, stars with just one period in their *K2* data are shown as black dots, and stars with more than one period are shown as open, red circles. For $(V - K_s)_0 < 3.5$, there is little or no preference for the stars with multiple periods to lie within the expected locus of single or binary stars. However, for $(V - K_s)_0 > 3.5$, the stars with more than one period are with very few exceptions displaced well above the single-star locus, thus supporting the interpretation that these are indeed binary stars.

rotate faster, on average, than the single stars in Upper Sco and probably in the Pleiades.

Collapsing the distributions into period histograms makes the difference between the single stars and the binaries somewhat more obvious. Histograms for the four clusters are provided in Figure 8. The Upper Sco histogram now clearly reveals that the binary stars are more weighted to short periods than the stars with just one *K2* period. The histogram for binaries and singles in Praesepe/Hyades, however, shows that those two distributions are very similar. These qualitative conclusions are confirmed by applying the KS test to the rotation data for the $M < 0.32\,M_{\odot}$ dM stars in the three clusters. This test reveals that the probability that the binary and single star rotation periods in Upper Sco are drawn from the same parent population is less than one part in 10^5; for the Pleiades, the probability is less than one part in 10^4. However, for Praesepe/Hyades, the KS test yields $p \sim 0.12$, indicating that the singles and binaries are consistent with being drawn from the same parent population.[11]

[11] There is a strong correlation between mass or $(V - K_s)_0$ color and period in these four clusters, potentially affecting these KS tests. As long as the distribution in color or mass for the binary and single stars is about the same, which is indeed the case, this should not greatly affect the KS test results. However, to be certain, we have also fit and removed the trend of median period as a function of color from the data for each cluster and repeated the KS test analyses. In all cases, these KS test probabilities confirm the original ones, with the same or higher degrees of significance.

Another way to emphasize the difference in rotation rates of binary and single stars in the three populations is to isolate the most rapidly rotating and most slowly rotating stars and ask what fraction of those stars are in binaries and what fraction are in singles. In Upper Sco, 41% (132/323) of all the $M < 0.32\,M_{\odot}$ stars are in *K2* binaries; however, among the 20% most rapidly rotating of the whole sample, 67% are in *K2* binaries, whereas among the 20% most slowly rotating stars, 36% are in *K2* binaries. In the Pleiades, 30% of all the late dM stars are in *K2* binaries, but 49% of the 20% most rapidly rotating stars are in *K2* binaries, and 12% of the 20% most slowly rotating stars are in *K2* binaries. Finally, for Praesepe/Hyades, 28% of all of the stars are in *K2* binaries, while 38% of the 20% most rapidly rotating stars are in *K2* binaries, and 25% of the 20% most slowly rotating stars are in *K2* binaries. These data show that binary stars are overrepresented among the most rapidly rotating stars in each cluster and underrepresented among the most slowly rotating stars, and that this bias is strongest at young ages.

Thus, assuming that the stars in these four clusters can be viewed as different snapshots in time of a single population, the rotation periods of the $M < 0.32\,M_{\odot}$ binaries are faster at very young ages than their single cousins, but angular momentum loss mechanisms apparently drive those rotation distributions to become more similar over time.

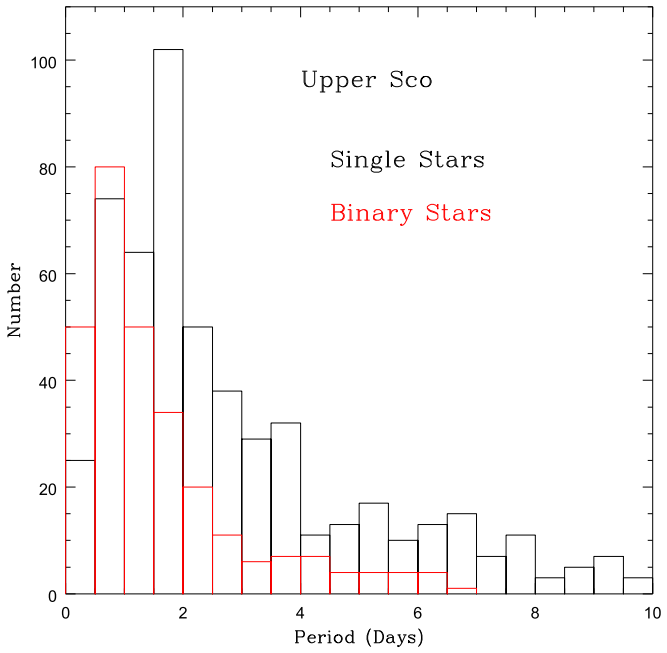

Figure 3. Histogram of the rotation periods for both components of the *K2* binary stars with $4.0 < (V - K_s)_0 < 6.5$ dM stars (roughly M0–M5.5) in Upper Sco compared to the rotation periods of the single dMs for the same color range (black line = single stars; red line = binary stars). The binary stars are clearly more rapidly rotating.

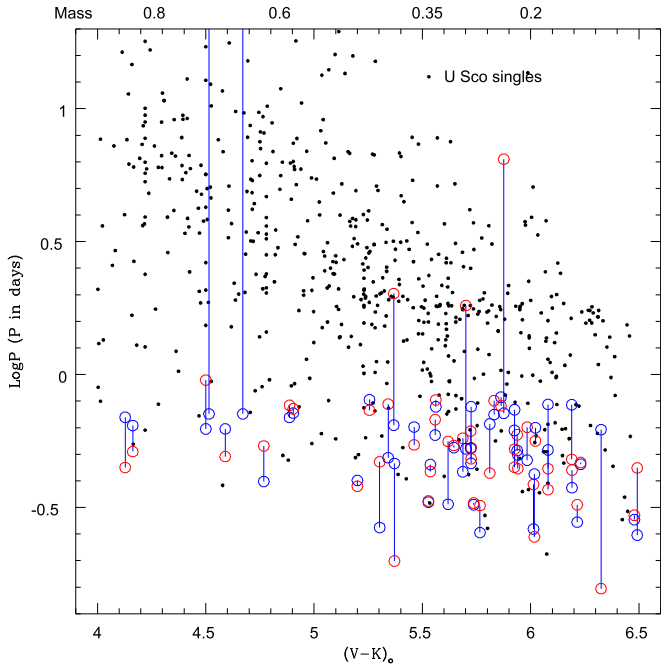

Figure 4. Period–color plot for the Upper Sco dM stars. Red and blue circles connected by a bar are the periods for the two components of a binary star; shown here are just the 50 most rapidly rotating (based on the period of the primary star) binaries. Black dots are the periods of the stars with just one detected period in our *K2* data. The primary star (blue circle) in each binary plotted here was chosen to be very rapidly rotating, but the secondary (red circle) could have had a period anywhere within the region spanned by the black points in the diagram. The fact that the secondaries nearly all have periods quite close to that of the primary is a new and (perhaps) unexpected result.

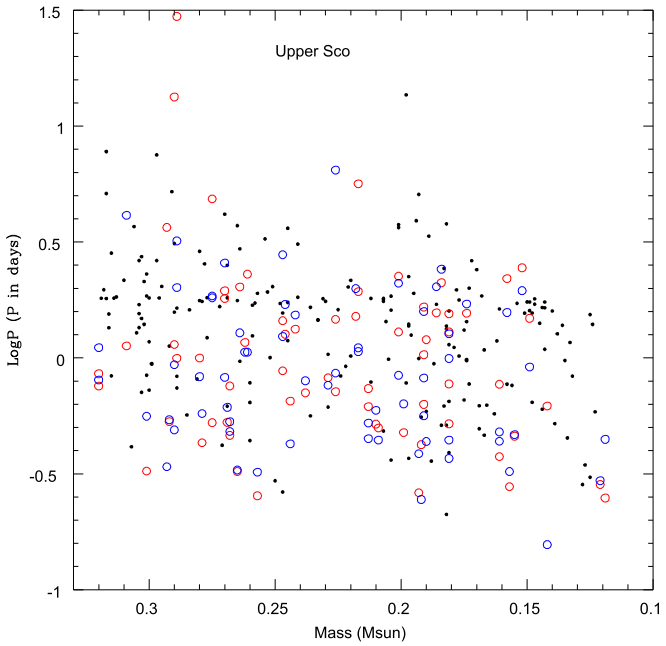

Figure 5. Correlation between rotation and mass for Upper Sco M dwarfs with $M \leqslant 0.32\,M_\odot$ and with *K2* rotation periods. The blue and red circles correspond, respectively, to the periods of the primary and secondary components of the *K2* binaries; the black dots mark periods for the stars identified as single by their *K2* data. The binary stars identified with the *K2* data dominate the most rapidly rotating part of the distribution, while single stars dominate the most slowly rotating region of the diagram.

5. Monte Carlo Simulations and Other Statistical Measures

In order to more fully compare the rotation periods of the late dM binaries in our four clusters to the single dMs, we have created a Monte Carlo simulation routine. For each run, the routine produces a simulated set of binary star periods drawn from the periods of the single stars, with the number of simulated binaries being the same as the actual number of binaries in that cluster. Because the companions we detect with *K2* must have magnitudes that are relatively similar to that of the primary, for each simulated binary we restrict the second period to come from a star within 0.15 mag in $(V - K_s)_0$ from the star selected randomly as the primary. For each binary star, we calculate a normalized period difference defined as $dP_n = |P_1 - P_2|/[(P_1 + P_2)/2]$. For the ensemble of simulated binaries in a given run, we derive the median normalized period difference and the median period for the primary star. We run 1000 such simulations for each cluster. Figure 9 compares the median normalized period and median first period for the actual set of binaries in each cluster to the median results for each of the 1000 simulations. The red star symbols in each of the plots denote the median primary period and median normalized period difference for the actual dM binaries in each cluster. The size of those symbols was chosen to provide a rough estimate of the statistical uncertainty in those values. Because the distributions of period and the normalized period differences are not Gaussian in shape, we cannot estimate those uncertainties as simply the standard deviation about the mean divided by the square root of the number of binary stars. Instead, we define $\pm 1\sigma$ as the range about the median in period (or normalized period difference) within which 67% of the

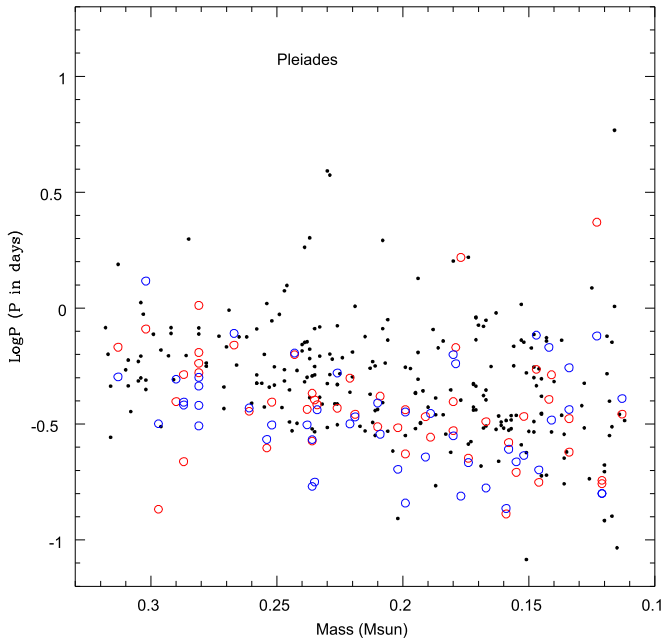

Figure 6. Correlation between rotation and mass for Pleiades M dwarfs with $M \leqslant 0.32\,M_{\odot}$ and with *K2* rotation periods. The stars that are components of binary stars identified with the *K2* data dominate the most rapidly rotating part of the distribution. (Notation is as in prior figure.)

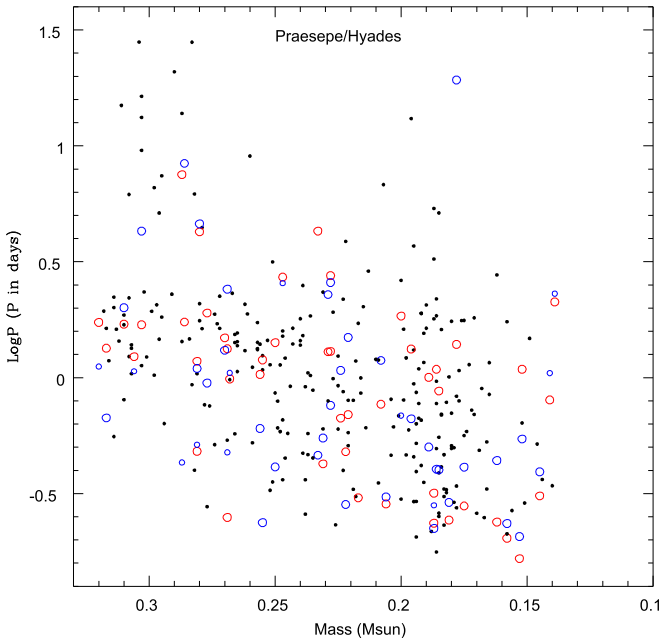

Figure 7. Correlation between rotation and mass for Praesepe/Hyades M dwarfs with $M \leqslant 0.32\,M_{\odot}$ and with *K2* rotation periods. The stars that are components of binary stars and the single stars do not obviously have different distributions in this diagram. (Notation is as in prior figure.)

values fall, and then we assume that the uncertainty in the median scales with the square root of the number of points.

The simulations confirm that the actual mid-dM *K2* binaries in Upper Sco and the Pleiades have periods that are shorter and closer to each other than the simulated populations drawn from the single stars. The Praesepe/Hyades mid-dM *K2* binaries have periods consistent with having been drawn from their single-star population.

6. The Influence of Disks

In standard models of the angular momentum evolution of low-mass stars, a common way to explain the presence of both slowly rotating and rapidly rotating populations at young ages is to include the influence of primordial circumstellar disks on stellar rotation (Königl 1991; Bouvier et al. 1997; Sills et al. 2000). When the disks are still present and actively accreting, they can drain angular momentum from the star and keep it slowly rotating. This could be tied to a difference in the rotation rate of single and binary stars if the binary stars are close enough to each other to disrupt or truncate a circumstellar disk that might be present around one or both components of the binary. In Rebull et al. (2018), we presented some direct evidence that "disk locking" is at work in at least a few of the Upper Sco stars with disks (classical T Tauris, CTTs), and that the low-mass CTTs do rotate more slowly than the WTT stars without IR excesses. Here we provide additional evidence that disks seem to have a particularly strong and deterministic influence on the rotation rates of $M < 0.32\,M_{\odot}$ stars in Upper Sco.

The rotation period histogram for Upper Sco shown in the left-hand panel of Figure 8 includes all members in that mass range. Rebull et al. (2018) identified 56 of those stars as possessing IR excesses consistent with primordial disks and hence their being CTTs. In Figure 10, we replot the Upper Sco rotation period histograms for single and binary mid-dM stars, but this time also marking those stars that have IR excesses. The disked stars have periods strongly peaking around 1–2 days. Comparing only the stars without IR excesses, the histograms for the single and binary stars are significantly more similar; a KS test now yields $P \sim 0.059$, indicating these two distributions are consistent (though only marginally) with having been drawn from the same parent population.

Figure 11 shows these same data in another way, also intended to highlight the link between IR excesses and rotation for very low mass stars in Upper Sco, as well as the strikingly narrow range in periods for the $M < 0.32\,M_{\odot}$ Upper Sco CTTs. In this plot of period versus $(V-K_s)_0$ color for just the Upper Sco CTTs, there appears to be a sharp transition at $\sim 0.4\,M_{\odot}$ ($(V-K_s)_0 \sim 3$), with a wide range in rotation periods for higher masses and a quite narrow range in rotation periods below that mass. If this is due to magnetohydrodynamic processes linking the star and the inner disk, then plausibly there is some change in either disk properties or magnetic field properties at that mass boundary. We have looked at the SEDs of the CTTs above and below the boundary mass, and we do not see any systematic differences (there is a range of SED shapes from transition disk to full Class II in both mass ranges). This could, therefore, be a signature of a change in magnetic field topology near this mass at Upper Sco age.

7. Additional Thoughts on Binarity and Rotation in Upper Sco and the Pleiades

If binarity links to rotation by suppressing star–disk angular momentum regulation, then knowledge of the orbital separation between the components of the binary becomes an important topic. Unfortunately, the $M < 0.32\,M_{\odot}$ stars in even these relatively nearby clusters are quite faint, and there is little published literature on their orbital periods or separations. However, if one opens up the topic to all dM members, then

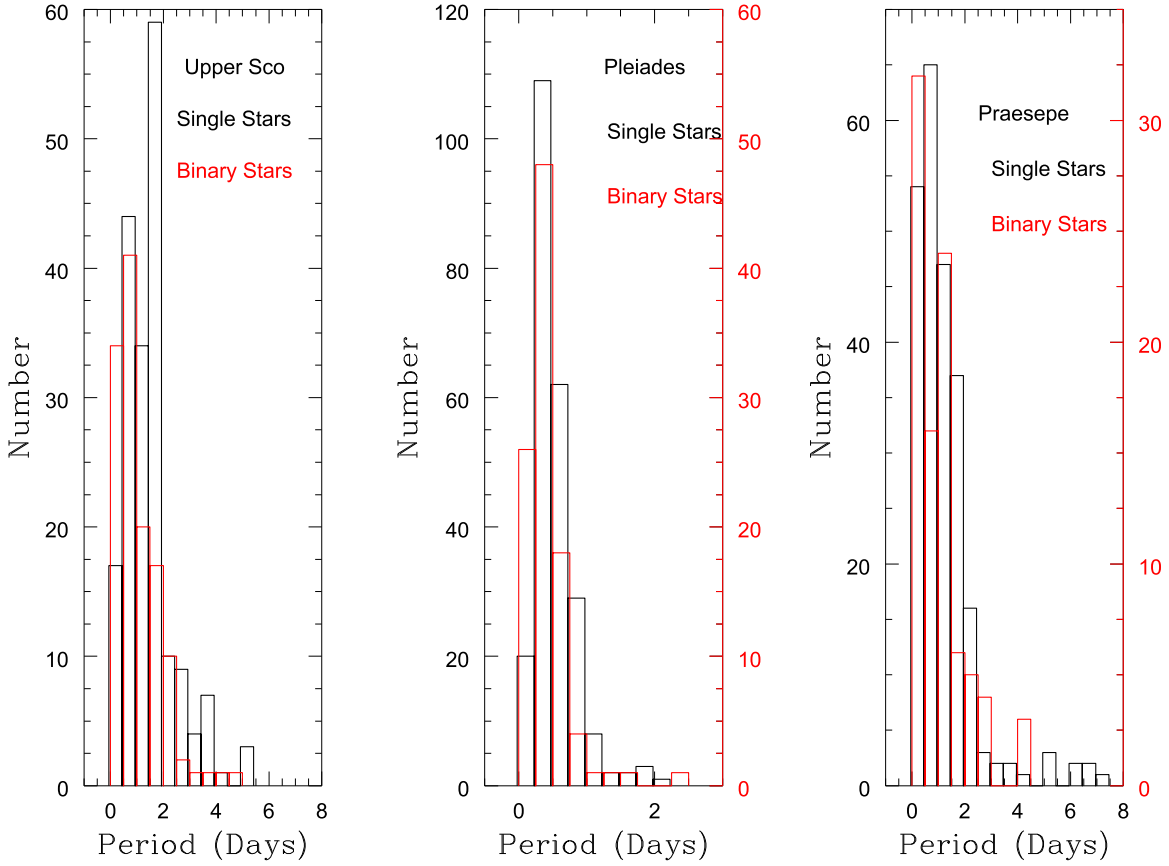

Figure 8. For stars with inferred masses $<0.32\,M_{\odot}$, a histogram comparison of the rotation periods for *K2* binary stars versus stars with only one rotation period in the *K2* data (hence assumed to be single or a low-q binary). At young ages, the binary stars are weighted toward rapid rotation compared to the single stars. At Praesepe age, the distributions for the singles and binaries appear, by eye, to be more similar. For the Pleiades and Praesepe, separate y-axis scales are used for the singles (left axis) and binaries (right axis) because there are only half as many binary star periods as there are single star periods.

there is more published literature, particularly for Upper Sco, where its youth makes the M stars comparatively bright.

The two most extensive and sensitive high-spatial-resolution imaging studies of Upper Sco (Kraus et al. 2008; Lafreniere et al. 2014) include 20 spectral type K7 or later members with *K2* data. One additional M2.5 *K2* member was observed with Keck LGS-AO by Ansdell et al. (2016). The pertinent data for these 21 stars are provided in Table 1. The reddest of these stars has $(V-K_s)_0 = 5.46$, corresponding to essentially $M = 0.32\,M_{\odot}$, reinforcing the claim that for $M < 0.32\,M_{\odot}$, there is little published high-spatial-resolution imaging data. However, for earlier type dM members of Upper Sco, the data in Table 1 indicate the following:

1. None of the AO binaries with $\Delta K > 1.0$ mag are detected with two periods by *K2*, in agreement with the belief that *K2* is detecting primarily "high-q" systems.
2. Four of the five AO binaries with $\Delta K < 0.2$ mag do have two periods detected by *K2*, also supporting that notion.
3. Essentially half of the AO binaries are also *K2* binaries.
4. Nine of the 10 *K2* binaries have $\Delta K \leqslant 0.6$ mag. Eight of the *K2* binaries have angular separation $<0\farcs33$ (projected spatial separation <45 au).

The AO data are therefore generally supportive of the idea that our *K2* dM binaries in Upper Sco (and presumably Pleiades and Praesepe) are binaries with high q and relatively small separation. However, because of the very poor overlap with our $M < 0.32\,M_{\odot}$ primary data set, any more definitive conclusions must await deeper, higher-spatial-resolution data.

The other avenue we can pursue with existing data is to ask "Why do we not detect two periods for all of the photometric binaries that lie well above the single-star locus in the optical CMDs for these clusters (see Figure 2)?" Perhaps our *K2* binaries are biased to short periods (relative to the full set of binaries), and the correlation we see between binarity and rotation is thus illusory. We cannot address this issue with Upper Sco data because the uncertainties in the dereddened colors are too large (specifically, we cannot identify a reliable photometric binary sample); therefore, we will use the Pleiades data. We make these tests for the full set of Pleiades dM stars $(4.0 < (V-K_s)_0 < 6.5)$ for which we have *K2* data in order to have as large a sample size as possible. First, we have compared the rotation periods of the photometric (but not *K2*) dM binaries with $\Delta V > 0.4$ mag to the dominant rotation periods of the *K2* dM binaries. Those two distributions are very similar; a KS test yields $p = 0.42$, indicating that the two distributions are consistent with having been drawn from the same parent population. Next, we compared the rotation periods of those same photometric (but not *K2*) binaries to the rotation periods of the dM stars lying within 0.25 mag of the single-star locus in the V versus $(V-K_s)_0$ CMD. That KS test yields $p = 0.0159$, indicating the two sets of stars are not

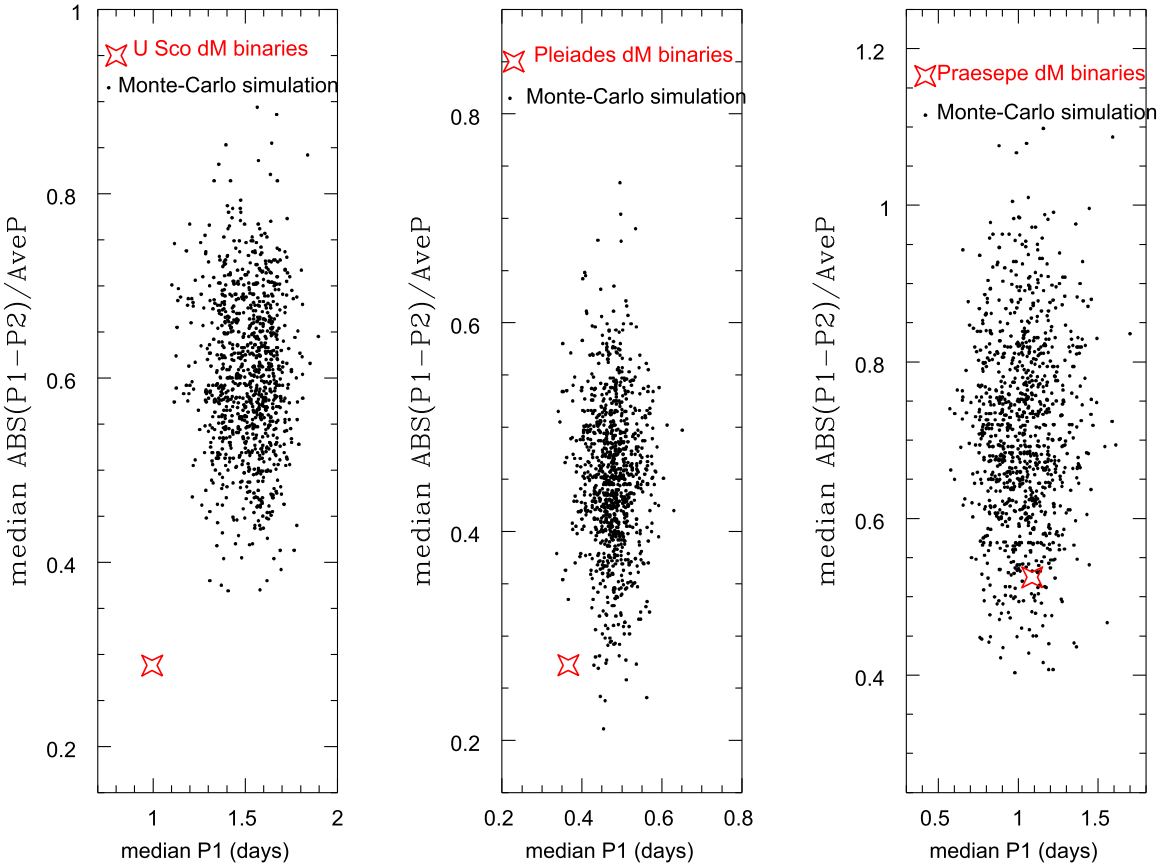

Figure 9. Comparison of the median P_1 and median normalized period difference for the actual *K2* dM binaries in our four clusters versus the same data for simulated binary populations drawn at random from the single-star periods. Each black dot represents the result of one simulation; each simulation creates the same number of binary stars as we have found in our *K2* data for that cluster, with the two periods drawn at random from the single-star population whose $(V - K_s)_0$ colors are within 0.15 mag of one of our binaries. We ran 1000 simulations for each cluster (resulting in the 1000 black dots for each cluster in the figure).

drawn from the same parent population, with the *K2* single but photometric binary stars rotating faster than the photometric single stars. We conclude from this that the dM stars in the Pleiades that are photometric binaries but where we detect just one *K2* period are also relatively rapidly rotating. We suspect that the reason we do not detect a second period in these systems is not due to any single cause, but could include secondaries that are nearly pole-on, or stars that just happen to have relatively axisymmetric spot distributions, or systems where the two periods are so close together we cannot separate them in the LS periodogram, or where the quality of the *K2* data are poorer than usual. We discuss these topics at length in the last section of the appendix.

8. Conclusions and Path Forward

We have used the excellent photometric time series light curves from NASA's *K2* mission to ask the question, "Are the rotation rates of the components of very low mass binary stars different from that of their similar-mass single stars at young ages?" The answer to that question is yes, at least for photometric binaries. Late-type dM stars in Upper Sco and the Pleiades with two detected periods (which we call "*K2* binaries") have rotation periods distinctly shorter than single stars of that mass. We have also shown that the rotation periods of the two stars in these binaries are significantly more similar to each other than would be true if the periods were drawn at random from the single-star population. These facts could in principle be due to at-formation processes whereby the components of the binary stars began their lives with more angular momentum than single stars. Or, it could result from angular momentum regulation mechanisms at young ages that might be influenced by the presence or absence of a companion star. We believe the latter explanation is more likely, based on our demonstration that much of the difference in the rotation period distributions for the single and binary dM stars in Upper Sco is due to a population of (relatively) slowly rotating CTTs. A plausible physical explanation of the slow rotation of the single dM stars is, therefore, that those stars retained their primordial circumstellar disks for a longer period and that disk locking (Königl 1991) or some similar process allowed them to drain away some of their angular momentum. The binary dM stars disrupt their disks and thus spin up more during PMS contraction.

By comparing populations of low-mass dM stars at three ages (8, 125, and 700 Myr), we have shown that the difference in rotational properties between the single and binary stars decreases with increasing age. This must arise as a result of the detailed dependence of angular momentum loss from winds on rotation rate for stars in this mass range (0.1–0.3 $M_\odot$). We intend to examine this topic in more detail in a future paper (M. Pinsonneault et al. 2018, in preparation).

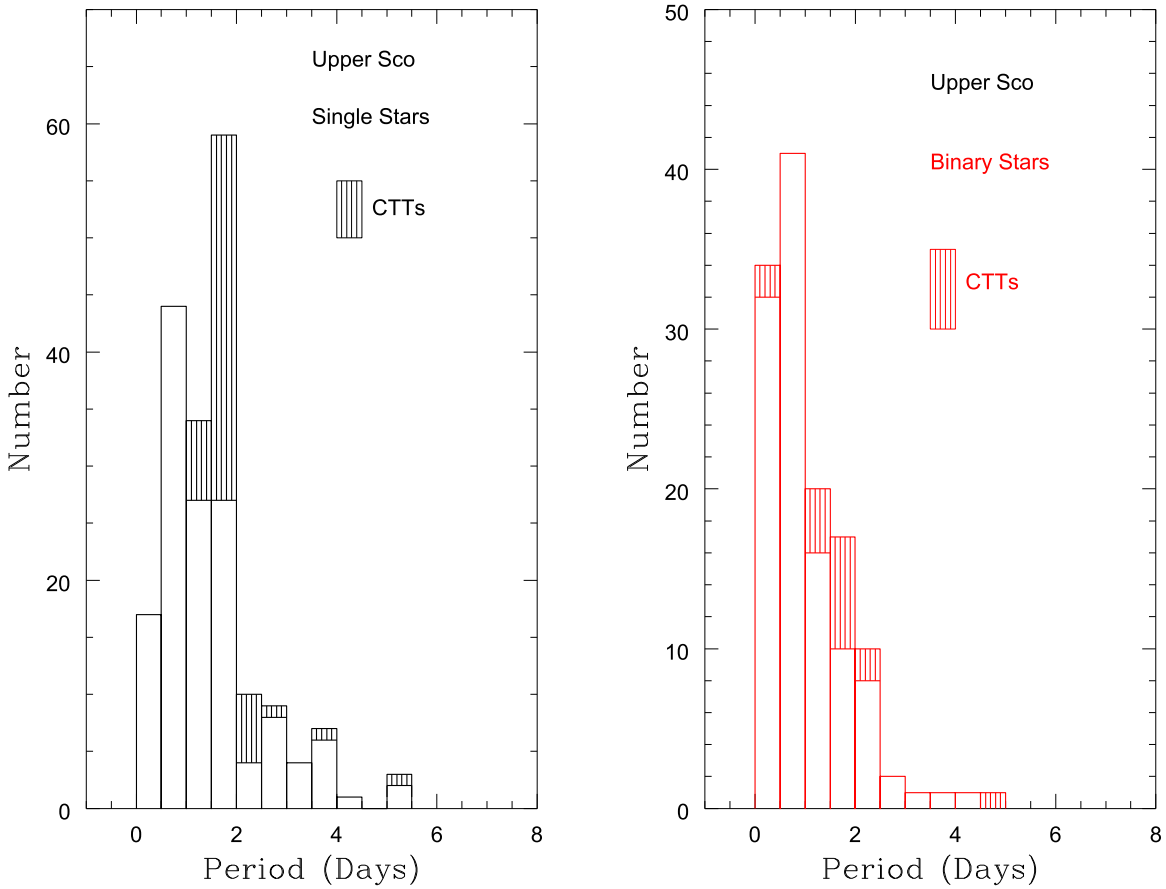

Figure 10. Same data as plotted in Figure 8 for Upper Sco, except now marking the stars that we believe to have IR excesses (with vertical hash marks), and therefore likely to have ongoing accretion. The left-hand panel shows the rotational period distribution for single mid-dMs; the right-hand panel shows the distribution for both components of the *K2* binary mid-dMs (there are eight binary systems with IR excess, so 16 of the periods in the right-hand plot are associated with CTTs). A large part of the difference between the binary and single star rotational distribution is due to the slowly rotating population of stars with IR excesses.

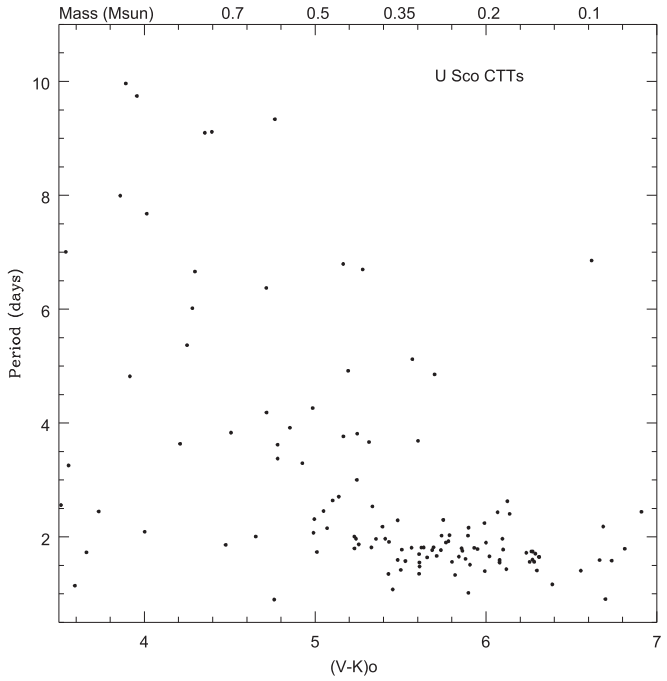

Figure 11. Rotation periods for just the Upper Sco CTTs for which we have *K2* data. Here, $M = 0.32\,M_{\odot}$ corresponds approximately to $(V - K_s)_0 = 5.3$. Redward of that color, the great majority of the CTTs have periods between 1 and 2 days; blueward of that color, there is a much wider range of rotation periods.

We note that our detection method probes only binaries with masses close enough for us to be able to measure the rotation periods of both components. Binaries with higher mass ratio could in principle have different rotation distributions, and it will be difficult to infer the spin rates of the secondaries in such systems. Our working hypothesis is that the difference in rotation rates is more logically tied to orbital period than to mass ratio, and that we see an effect because binaries with low mass ratios are more likely to be close. A testable prediction would therefore be that we would expect wider binaries to have rotation rates similar to single stars. The most important next step in order to use the very low mass stars in these clusters to help us better understand the formation and evolution of single and binary stars will be to obtain high-spatial-resolution imaging and multiepoch radial velocity data in order to determine or constrain the separations (or orbital periods) and mass ratios of the binary stars in our four clusters, with the most important targets being the younger (Upper Sco and Pleiades) stars. In Upper Sco, in particular, it may be possible to use *Gaia* DR2 data to determine a better member list and to more accurately plot stars in a CMD by providing accurate individual distances. Spectra of sufficient quality to determine quantitative spectral indices could provide a better means to produce an equivalent CMD and (with *Gaia* DR2 distances) thereby yield a photometric binary sequence with quality similar to that of the older clusters.

Table 1
Upper Sco dM Binaries with Both AO and *K2* Data

EPIC Number	Spectral type	P_1 (days)	P_2 (days)	ΔK_s[a] (mag)	Separation[a] (arcsec)	Name
205089832	M2	8.1750	⋯	1.59	0.092	USco 160707.7–192715
205060410	M1	17.9258	⋯	0.98	0.652	USco 160823.8–193551
205137430	K7	12.2019	⋯	3.83	5.775	USco 161031.9–191305
204251947	M1	5.4849	⋯	0.37	1.981	GSC 06793–00868
204342099	M1	⋯	⋯	1.19	1.907	GSC 06793–00806
204179058	M1	3.0039	0.5857	0.78	0.054	ScoPMS 017
204436170	M1	0.8621	0.7271	0.03	0.025	ScoPMS 019
205167008	M3	4.1422	⋯	2.48	4.61	ScoPMS 042b
204878974	M1	3.0938	0.8548	0.43	0.189	RX J1600.5–2027
204794876	M0	1.4900	2.1528	0.58	0.205	RX J1601.7–2049
203834337	K7	4.6547	⋯	1.00	0.076	RX J1601.8–2445
204894575	K7	1.9540	⋯	0.18	0.310	RX J1602.9–2022
204862109	M0	1.7281	1.0520	0.53	0.121	RX J1603.9–2031B
205142483	M1	6.6342	⋯	1.47	0.599	RX J1607.0–1911
204040060	M0.5	7.2390	⋯	0.63	1.324	ScoPMS 016
204406748	M3	4.3922	16.9554	0.60	0.193	ScoPMS 020
205164892	M1	6.6595	⋯	0.42	0.299	ScoPMS 042a
203895983	M2.5	2.4474	2.5757	0.1	0.298	RIK 77
203628765	M0	0.5034	0.6615	0.07	0.594	[PZ99] J155716.6–252918
205087483	M4	1.5134	2.3752	0.05	0.862	[PGZ2001] J160801.5–192757
205374937	M4	0.6345	0.5436	0.05	0.098	[PGZ2001] J161118.1–175728

Note.
[a] The ΔK and separation data are from Kraus et al. (2008), Lafreniere et al. (2014), and Ansdell et al. (2016).

Some of the data presented in this paper were obtained from the Mikulski Archive for Space Telescopes (MAST). Support for MAST for non-*HST* data is provided by the NASA Office of Space Science via grant NNX09AF08G and by other grants and contracts. This paper includes data collected by the *Kepler* mission. Funding for the *Kepler* mission is provided by the NASA Science Mission directorate. This research has made use of the NASA/IPAC Infrared Science Archive (IRSA), which is operated by the Jet Propulsion Laboratory, California Institute of Technology, under contract with the National Aeronautics and Space Administration. This research has made use of NASA's Astrophysics Data System (ADS) Abstract Service and of the SIMBAD database, operated at CDS, Strasbourg, France. This research has made use of data products from the Two Micron All-Sky Survey (2MASS), which is a joint project of the University of Massachusetts and the Infrared Processing and Analysis Center, funded by the National Aeronautics and Space Administration and the National Science Foundation. The 2MASS data are provided by the NASA/IPAC Infrared Science Archive, which is operated by the Jet Propulsion Laboratory, California Institute of Technology, under contract with the National Aeronautics and Space Administration. This publication makes use of data products from the *Wide-field Infrared Survey Explorer*, which is a joint project of the University of California, Los Angeles, and the Jet Propulsion Laboratory/California Institute of Technology, funded by the National Aeronautics and Space Administration.

Facility: K2, Exoplanet Archive, IRSA, 2MASS.

Appendix A
Mass Estimates

In order to make the best comparison of rotation properties between the three age bins, it is desirable to select samples of M dwarfs in each cluster that span the same mass range. This is relatively straightforward for the Pleiades, Hyades, and Praesepe, where all of the stars of interest are on or close to the ZAMS and where theoretical isochrones have been well calibrated from comparison to empirical data. However, for Upper Sco, the theoretical models are known to have issues, and there are significant disagreements between models. Related to these issues with the models, the age of Upper Sco is a subject of significant debate, and that directly impacts any stellar mass estimates. It is also true that for the mass range of interest to this study, few—if any—of the theoretical models predict accurate $(V-K_s)_0$ colors for M dwarfs. This is a problem for us because we have used $(V-K_s)_0$ as our primary mass surrogate in all our papers on the *K2* open cluster data. Despite these issues, we have attempted to derive reliable mass estimates for the M dwarfs in the four clusters; we describe our methodology here.

Table 2
Properties of the Clusters

Cluster name	Age (Myr)	Distance (pc)	[Fe/H]	A_V (mag)
Upper Sco	8 Myr	140	0.0	0.7
Pleiades	125 Myr	136	0.0	0.12
Praesepe	700 Myr	184	0.15	0.00
Hyades	700 Myr	46	0.15	0.00

It is first necessary to adopt fundamental parameters for the four clusters defining the cluster age, distance, metallicity, and reddening. These parameters are provided in Table 2. The values in Table 2 are those we used in our previous papers on the *K2* rotation data for these clusters (Rebull et al.

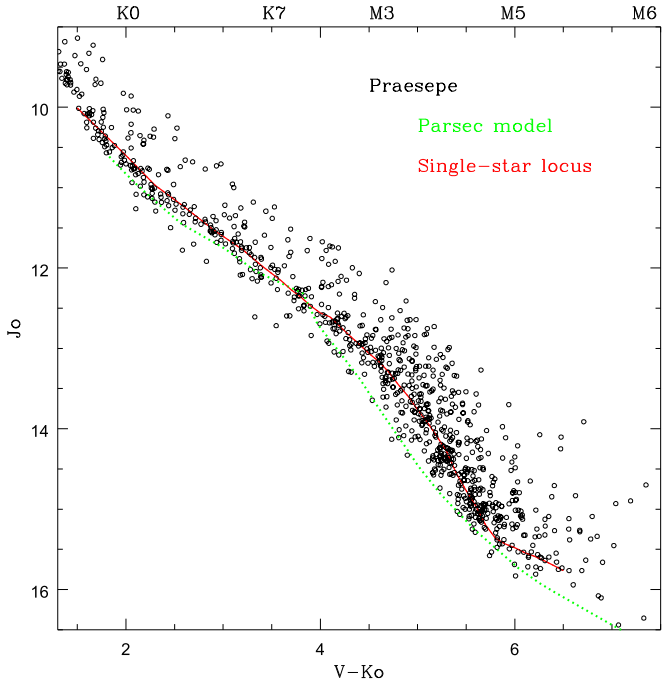

Figure 12. CMD for low-mass stars in Praesepe for which we have *K2* light curves. The red, solid curve is our empirical fit to the single-star locus. The green, dashed curve is the PARSEC 700 Myr isochrone, assuming a distance of 184 pc, no reddening, and [Fe/H] = +0.1 for Praesepe.

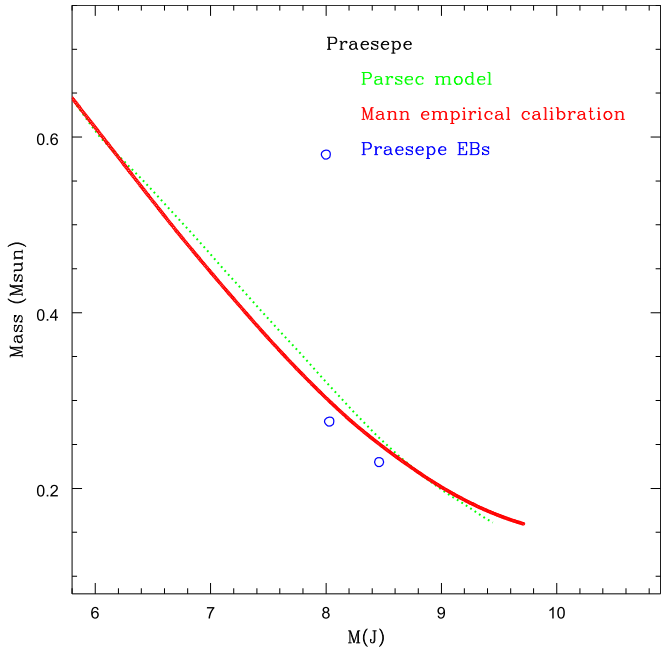

Figure 13. Comparison between the predicted mass–M_J correlation for low-mass stars based on the 700 Myr PARSEC isochrone and an empirical mass–M_J correlation based on the results of Mann et al. (2015).

2016a, 2017, 2018); references for the adopted ages, distances, and reddenings can be found in those papers. We adopt solar metallicities for Upper Sco and Pleiades since that is consistent with the overall literature for those clusters. Praesepe and the Hyades are generally considered to be somewhat metal-rich (Boesgaard & Budge 1988; An et al. 2007; Pace et al. 2008; Cummings et al. 2017); the [Fe/H] = +0.15 value we adopt is a compromise between the values reported in those papers.

For the Pleiades, Hyades, and Praesepe, we will use theoretical model isochrones to derive mass estimates based on observables. Based in part on arguments presented in T. David et al. (2018, in preparation) and in part on evidence provided below, we adopt the PARSEC models (Chen et al. 2014) for this purpose. We also will assume that Praesepe and the Hyades have similar enough properties that we can derive an M_J-to-mass transformation for Praesepe, and we use that same relation for the Hyades.

For Praesepe, we derive mass estimates in the following manner. First, we create a J versus $(V-K_s)_0$ color–magnitude diagram, as shown in Figure 12. The CMD has a well-defined single-star locus and a well-populated binary/triple sequence (stars that fall above the single-star locus by amounts up to about 1.0 mag, which would correspond to a triple system of nearly equal mass stars). We fit a curve to the single-star locus, as illustrated by the red line in Figure 12. We convert J magnitudes to M_J values using the distance and reddening in Table 2. For every star in the cluster, we assign it the M_J from this curve corresponding to its $(V-K_s)_0$. For binaries, this means that the mass we associate with the system corresponds approximately to the mass of the primary star. Figure 12 also includes a curve showing the location of the PARSEC 700 Myr isochrone in the J versus $(V-K_s)_0$ plane compared to the actual Praesepe photometry. While the overall match is fairly good, there is a significant discrepancy between the isochrone shape and the locus of Praesepe points among the M dwarfs. That discrepancy emphasizes why we do not simply use $(V-K_s)_0$ color as the link between the theoretical isochrone and mass.

As an empirical check on the masses we derive in this way, in Figure 13 we compare the masses inferred from the PARSEC model isochrone absolute J magnitude to masses inferred from the semiempirical mass–M_K relation derived in Mann et al. (2015) from field stars. We convert the Mann relation to mass–M_J using the observed $J-K_s$ colors of the Praesepe stars. Praesepe is old enough that even the lowest mass M dwarfs with *K2* photometry are essentially on the main sequence, so comparison to a field star relation should be valid. Figure 13 shows that the masses derived from the PARSEC isochrone absolute J magnitude are in good agreement with the Mann et al. relation, with maximum deviations of only a few hundredths of a solar mass. Finally, we also show mass/M_J points for two low-mass Praesepe eclipsing binaries identified from *K2* data (Gillen et al. 2017). One of these systems, AD2615, consists of two components with nearly equal mass; we plot the data point at the average mass and with $M_{J,\mathrm{primary}} = M_{J,\mathrm{system}} + 0.75$. The other system, AD3116, consists of a 0.276 $M_\odot$ primary and a brown dwarf secondary. We adopt $M_{J,\mathrm{primary}} = M_{J,\mathrm{system}}$ and plot the point at the mass of the primary star. We do not plot data for a third Praesepe EB, AD 3814 (Kraus et al. 2017), because the two stars have masses of 0.38 and 0.21 $M_\odot$, and there is no certain way to estimate the J magnitude of each component.

We followed essentially the same procedure for assigning masses to the low-mass stars in the Pleiades. Figure 14 shows the J versus $(V-K_s)_0$ CMD for the low-mass stars observed by *K2*. As for Praesepe, the PARSEC isochrone at Pleiades age provides a reasonably good fit to the observed photometry for

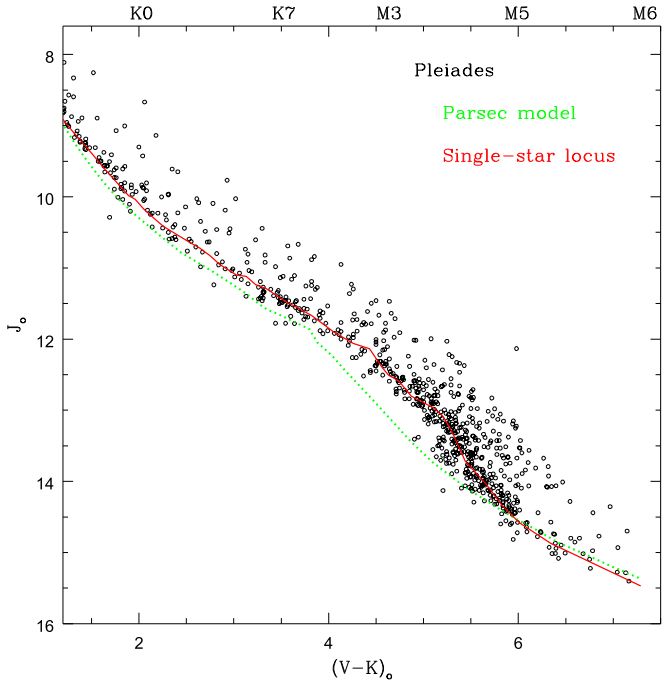

Figure 14. CMD for low-mass stars in the Pleiades for which we have *K2* light curves. The red, solid curve is our empirical fit to the single-star locus. The green, dashed curve is the PARSEC 125 Myr isochrone, assuming a distance of 136 pc, $A_V = 0.12$, and solar metallicity for the Pleiades.

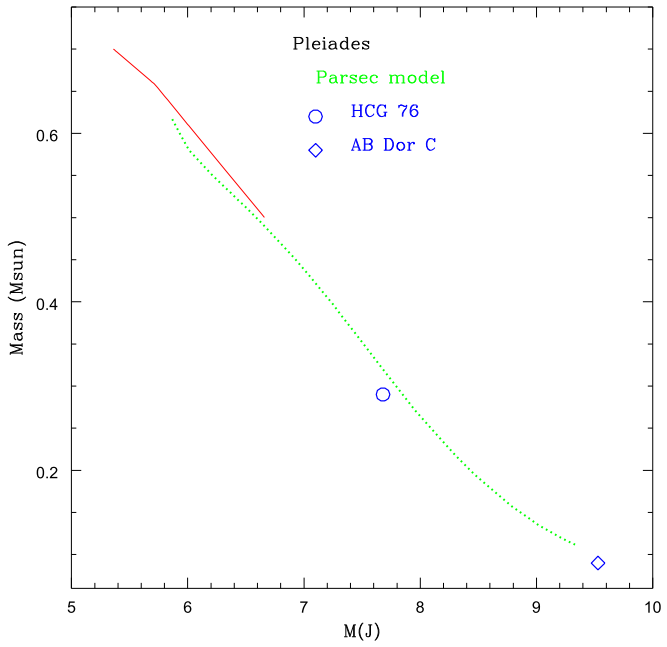

Figure 15. Comparison between the predicted mass–M_J correlation for low-mass stars based on the 125 Myr PARSEC isochrone and an empirical mass–M_J correlation based on the results of Mann et al. (2015). Also shown are direct mass estimates for the Pleiades dM member HCG 76 and for the Pleiades-age binary star AB Dor C.

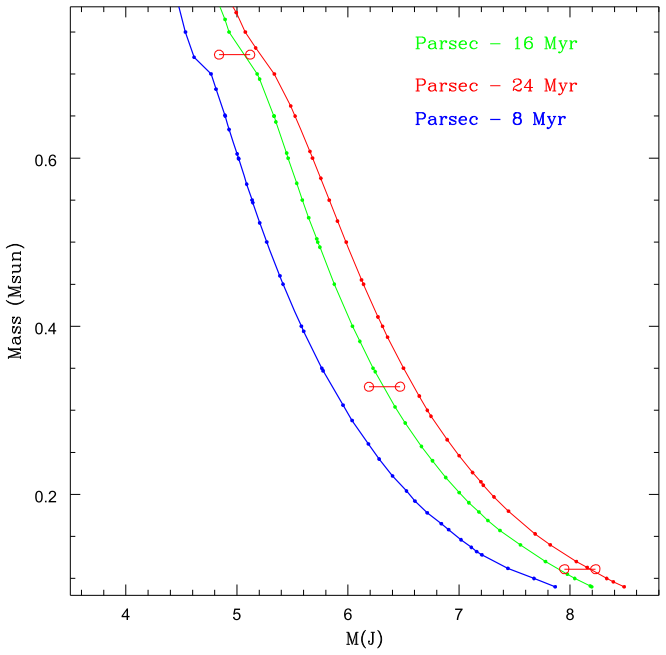

Figure 16. Comparison between the predicted mass–M_J correlation for low-mass stars based on the 8, 16, and 24 Myr PARSEC isochrones and data for three Upper Sco dM eclipsing binary stars with accurate masses (Kraus et al. 2015; David et al. 2016; T. David et al. 2018, in preparation). The EBs are plotted at both $A_V = 0.0$ and $A_V = 1.0$.

the K dwarfs and the late M dwarfs, but for $4 < (V - K_s)_0 < 5.5$, the isochrone is considerably too blue. Figure 15 shows the mass versus M_J plot for the Pleiades derived from the PARSEC 125 Myr isochrone. As empirical checks on this relation, we also plot as a solid red line the Mann et al. (2015) main-sequence relation for just the mass range where we expect the Pleiades stars to be on or very near the main sequence. We also plot the one Pleiades dM EB with accurate mass estimates where we can also estimate an appropriate M_J, HCG 76 (David et al. 2016). We additionally plot data for the Pleiades-age binary star AB Dor C (Luhman et al. 2005; Close et al. 2007; Azulay et al. 2017). These empirical checks confirm that our M_J-to-mass conversion derived from the PARSEC isochrone should provide reasonably accurate masses for the low-mass stars in the Pleiades.

Because theoretical isochrones at young ages are considerably more uncertain and because of the (related) uncertainty in ages of star-forming regions, we adopted a different procedure for assigning masses in Upper Sco. Instead of using the isochrone to define a conversion from M_J to mass and then using masses derived from binary systems as an empirical check, for Upper Sco we use the masses from binary systems to provide the basis for our M_J-to-mass conversion and use a theoretical isochrone only as a convenient interpolation scheme between the binary star data points. This is fortunately possible because there are three Upper Sco dM eclipsing binary systems with accurate masses and where the components of the binaries are nearly equal in mass (Kraus et al. 2015; David et al. 2016, 2018, in preparation). The data for these three systems are provided in Table 3.

Figure 16 plots the three Upper Sco eclipsing binaries (EBs) in the mass versus M_J plane and compares their locations to PARSEC isochrones for 8, 16, and 24 Myr. We plot the Upper Sco EBs at both $A_V = 0.0$ and $A_V = 1.0$; their actual A_V should lie somewhere within that range. For each star, we use the average of the two masses, and we add 0.75 mag to the observed J magnitude to get a magnitude corresponding to just one of the stars. It can be seen that the PARSEC isochrones have a shape in this plane similar to the three fiducial

Table 3
Properties of the Upper Sco dM Eclipsing Binaries

EPIC Number	Name	M_1 (M_{sun})	M_2 (M_{sun})	J (System) (mag)	Spectral type	References
204376071	UScо 48	0.737	0.709	9.824	M1	T. David et al. (2018, in preparation)
205030103	UScoCTIO 5	0.332	0.319	11.172	M4.5	Kraus et al. (2015), David et al. (2016)
203710387	⋯	0.116	0.106	12.932	M5	David et al. (2016)

Table 4
Upper Sco $M < 0.32\,M_\odot$ Stars with *K2* Periods

EPIC Number	$(V-K)_o$	P_1 (days)	P_2 (days)	Mass ($M_\odot$)	Disk?
202515599	6.460	0.5851	⋯	0.123	
202632400	6.073	1.3723	⋯	0.182	
202638454	6.492	0.2487	0.4455	0.119	
202709862	5.655	0.9952	2.0106	0.289	
202793212	5.590	2.1634	⋯	0.310	
202795175	5.883	0.8361	⋯	0.224	
202828127	6.388	1.1663	⋯	0.133	Y
202873945	6.161	0.6258	⋯	0.166	
202879519	6.011	5.0729	⋯	0.193	

(This table is available in its entirety in machine-readable form.)

Table 5
Pleiades $M < 0.32\,M_\odot$ Stars with *K2* Periods

EPIC Number	$(V-K)_o$	P_1 (days)	P_2 (days)	Mass ($M_\odot$)
210769047	5.705	0.6439	⋯	0.194
210791550	5.471	0.3727	⋯	0.248
210815768	5.867	0.2999	⋯	0.163
210822528	5.818	0.9149	⋯	0.171
210832378	5.462	0.4656	⋯	0.251
210833622	5.452	1.0465	⋯	0.254
210854098	6.079	0.3451	⋯	0.137
210860152	5.486	0.6299	⋯	0.243
210866482	5.482	0.3228	⋯	0.245
210871940	5.313	0.2773	⋯	0.316

(This table is available in its entirety in machine-readable form.)

Table 6
Praesepe/Hyades $M < 0.32\,M_\odot$ Stars with *K2* Periods

EPIC Number	$(V-K)_o$	P_1 (days)	P_2 (days)	Mass ($M_\odot$)	Cluster
210468157	5.515	1.3950	⋯	0.256	H
210540496	6.162	0.3409	⋯	0.178	H
210640966	5.554	2.7156	2.5569	0.247	H
210674207	5.469	0.9868	1.0488	0.268	H
210700098	5.361	2.3441	⋯	0.302	H
210742017	5.690	2.8806	⋯	0.213	H
210742592	5.341	0.8036	⋯	0.310	H
210744677	5.420	0.4813	0.5136	0.281	H
210754620	5.381	0.6339	⋯	0.294	H
210769813	5.340	1.8632	⋯	0.310	H

(This table is available in its entirety in machine-readable form.)

points, with the 16 Myr isochrone most nearly matching the three fiducials. Because it is thought that magnetic fields and starspots (not included in the PARSEC models) may significantly influence the observed isochrone magnitudes and colors, we are not advocating that this favors a 16 Myr age for Upper Sco. We simply advocate that the 16 Myr isochrone provides a convenient means to place our *K2* Upper Sco stars onto a mass scale that is consistent with the empirical data provided by the EBs.

Tables 4–6 provide the colors, periods, and mass estimates for the $M < 0.32\,M_\odot$ stars that are analyzed in the main text of the paper. The colors and periods are the same as originally reported in Rebull et al. (2016a, 2017, 2018).

Appendix B
Reality of the Spike in Upper Sco M Dwarf Rotation Periods near $P = 1.8$ days

Close examination of Figures 4 and 5 of Section 3 seems to show a peculiar linear, approximately horizontal structure for $5 < (V-K_s) < 6.5$ and periods near but slightly less than 2 days ($\log P = 0.3$). We worried that this might be a sign that some artifact in the *K2* data acquisition or pipeline processing was imposing this period on the data and therefore at least some of these periods are not real. We were particularly concerned about an artifact at or near $P = 2$ days, because that is the period at which *K2* dumps angular momenta that have built up in their reaction wheels (van Cleve et al. 2016). Small pointing jumps are thus likely to occur with that periodicity, which could be imprinted on the time series photometry.

We had noticed a concentration of periods near $P = 2.0$ days while preparing the data tables for Rebull et al. (2018). In fact, our original set of periods had even more stars near this period, making plots of period versus color appear even more anomalous. Therefore, in the context of Rebull et al. (2018), we reviewed extensively the light curves with periods between 1.5 and 2.5 days. We think it likely that there is indeed an instrumental or processing artifact near 2.0 days; see Figure 17 for four examples of light curves with apparent 2-day periods that we discarded as likely spurious (these periods were not reported in Rebull et al. 2018). Note that these phased light curves are almost discontinuous. They are also extremely low in amplitude. We, in fact, believe that the stars where one sees this 1.96-day instrumental period are almost exclusively stars that are intrinsically nonvariable. The imposed 2-day period only appears with a large enough signal to be detected in the LS periodogram for such nonvariable stars. Examination of the *K2* light curve data files shows that there are indeed small position shifts at the times when momentum dumps are flagged, and that these do occur at a 1.96-day cadence.

Figures 5 and 6 of Section 3 were constructed after our removal of all the stars we believed had instrumentally imposed

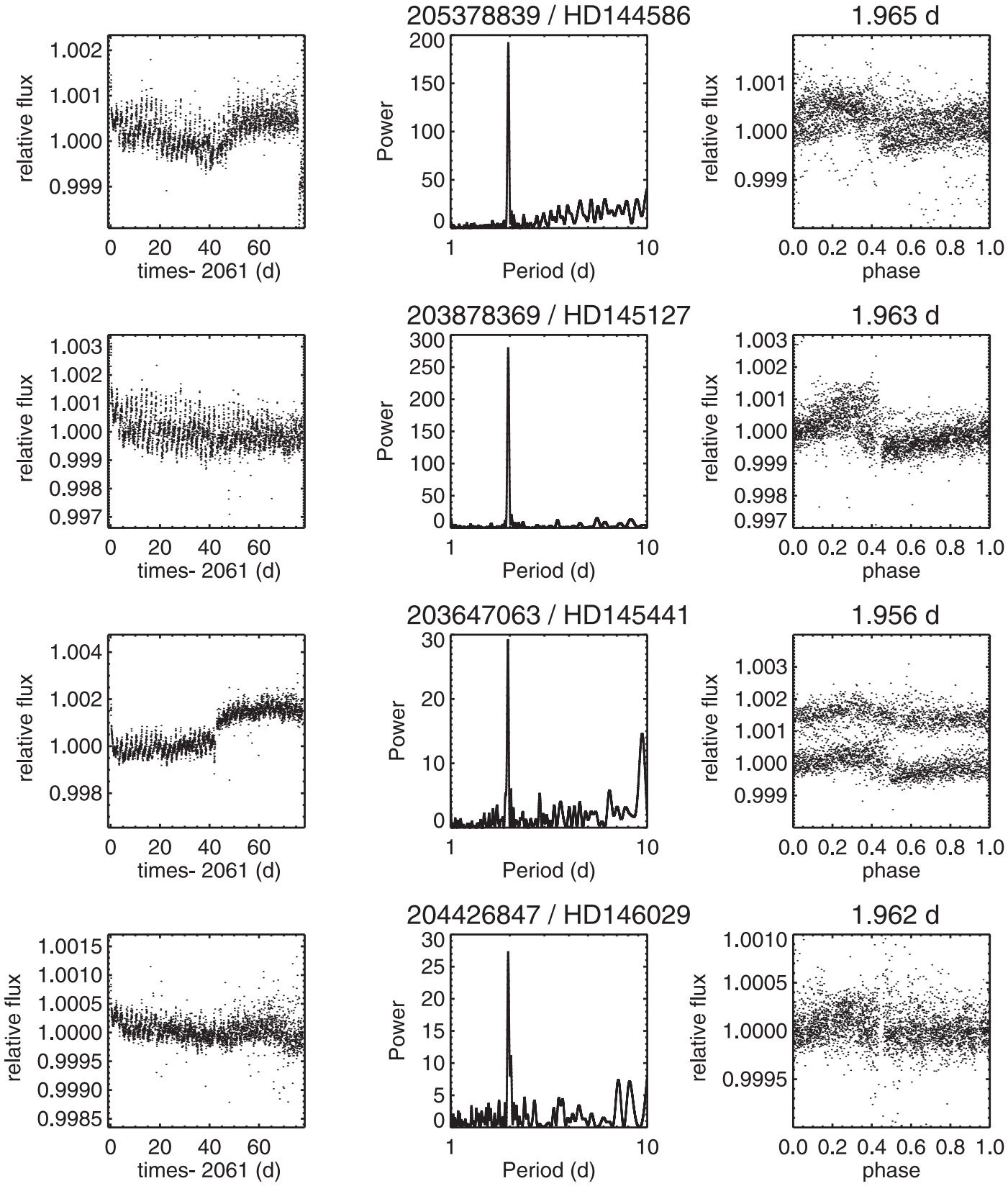

Figure 17. Four examples of light curves with spurious ∼2-day periods. First column: light curve; second column: power spectrum; third column: phased light curve for the ∼2-day period peak in the periodogram. Note the near discontinuity in the phased light curves, often coinciding with a small gap in the data. We discarded LCs with this kind of behavior as likely instrumental. Specific stars are EPIC 205378839/HD144586, EPIC 203878369/HD145127, EPIC 203647063/HD145441, and EPIC 204426847/HD146029.

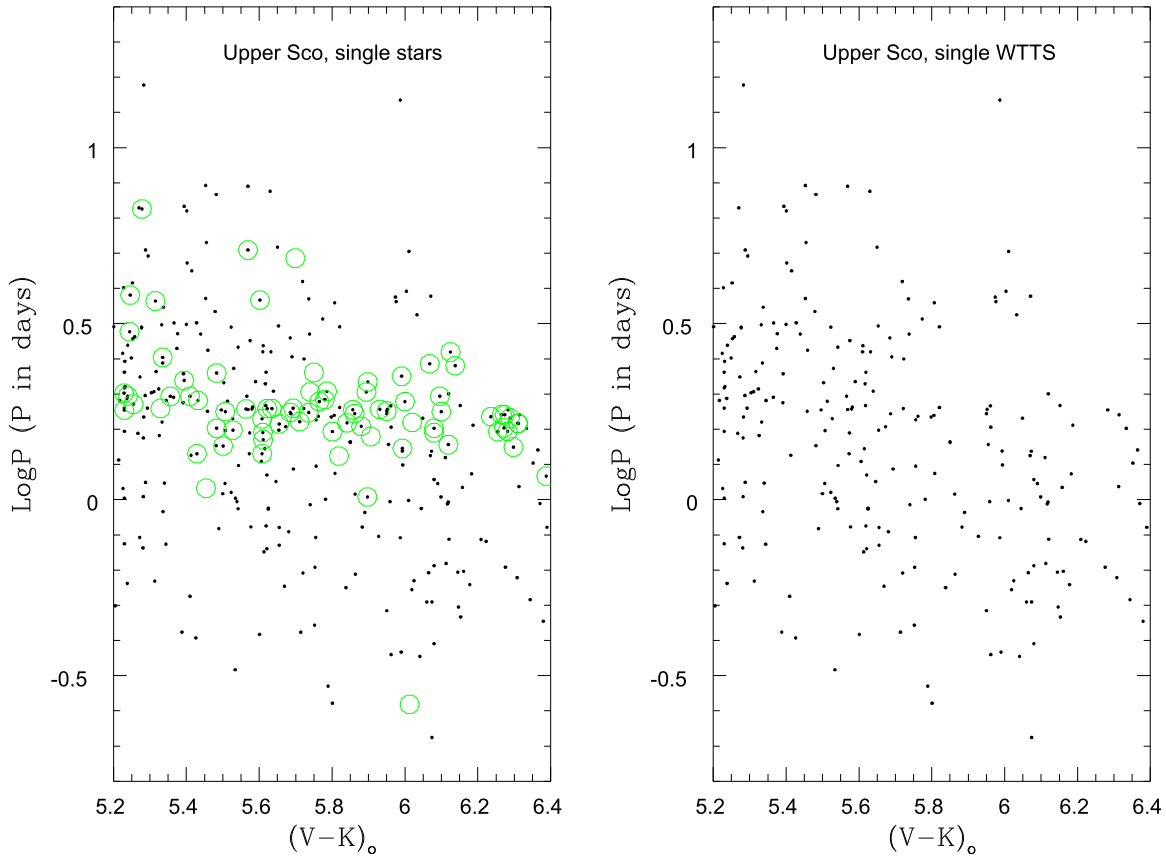

Figure 18. Left: periods for Upper Sco $M < 0.32\ M_{\odot}$ single stars, with black dots corresponding to stars without IR excesses and green circles corresponding to stars with IR excesses. The periods for the IR-excess stars (CTTs) concentrate around a period a little less than two days, whereas the stars without disks have a much more scattered period distribution. Right: same plot, but now plotting only the stars without IR excesses. There is no obvious concentration of points near log $P = 0.3$.

2-day periods. We believe that all of the periods we retained in Rebull et al. (2018) and that we have used in this paper are physical. One reason for this belief is that most or all of the remaining excess in periods near 2.0 days is attributable to CTTs; any instrumentally induced periodicity should have no knowledge of whether the star is a CTT or a WTT. We illustrate this point in Figure 18(a), which replots the Upper Sco rotation data for only stars with single *K2* periods, and where we highlight (as green circles) stars with certain IR excesses (i.e., they are CTTs). The CTTs are concentrated around $P \sim 1.8$ days (log P = 0.25). If one removes the CTTs from the diagram, as shown in Figure 18(b), there is no longer any significant hint of an excess.

In contrast to the stars with instrumentally imposed periods, Figures 19 and 20 show that stars that have intrinsic periods near ∼2 days have normal light curves for young, low-mass stars. Figure 19 has stars without disks, and Figure 20 has stars with disks. Note that the phased light curves are completely different than the ones in Figure 17, even for those stars with disks; the phased light curves are continuous, often sinusoidal.

Finally, we have fit a line to the periods for just the disked stars (using outlier-resistant linear fitting robust_linefit.pro from the IDL astro library) for $5 < (V - K_s)_0 < 6.4$ and $1 < P < 3$. The fit, shown in Figure 21, has a small but significantly nonzero slope (-0.0724 ± 0.0241). We also provide a dotted line in the figure at the instrumentally induced period of 1.96 days. There are three takeaways from this figure:

1. The CTT periods do not concentrate around the 1.96-day instrumentally induced period.
2. While the dM CTT periods are concentrated in a relatively small range in period, their dispersion in period is *much* larger than the uncertainty in the individual periods.
3. The CTT periods are a (weak) function of color, with longer mean periods at higher mass.

All three of those points argue against the apparent linear arrangement of periods in Figures 4 and 5 of Section 3 being an artifact, and instead argue that the preference for periods near 1.8 days for low-mass CTTs at Upper Sco age must be due to a physical process like the disk-locking mechanism of Ghosh & Lamb (1979).

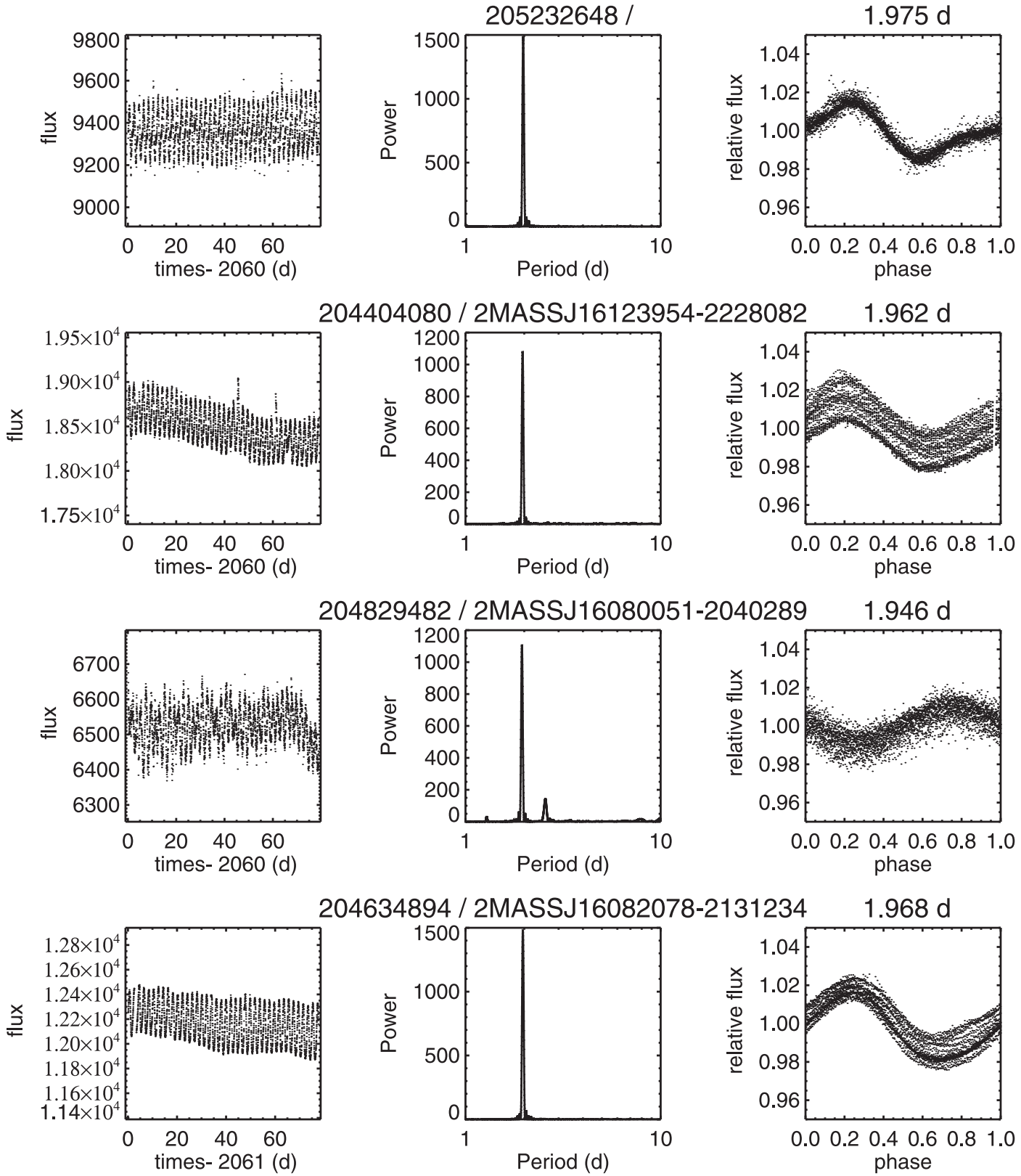

Figure 19. Four examples of light curves (from disk-free stars) with intrinsic ∼2-day periods. First column: light curve; second column: power spectrum; third column: phased light curve for the ∼2-day period peak in the periodogram. We retained LCs with this kind of behavior as likely real. Specific stars are EPIC 205232648, EPIC 204404080/2MASSJ16123954–2228082, EPIC 204829482/2MASSJ16080051–2040289, and EPIC 204634894/2MASSJ16082078–2131234.

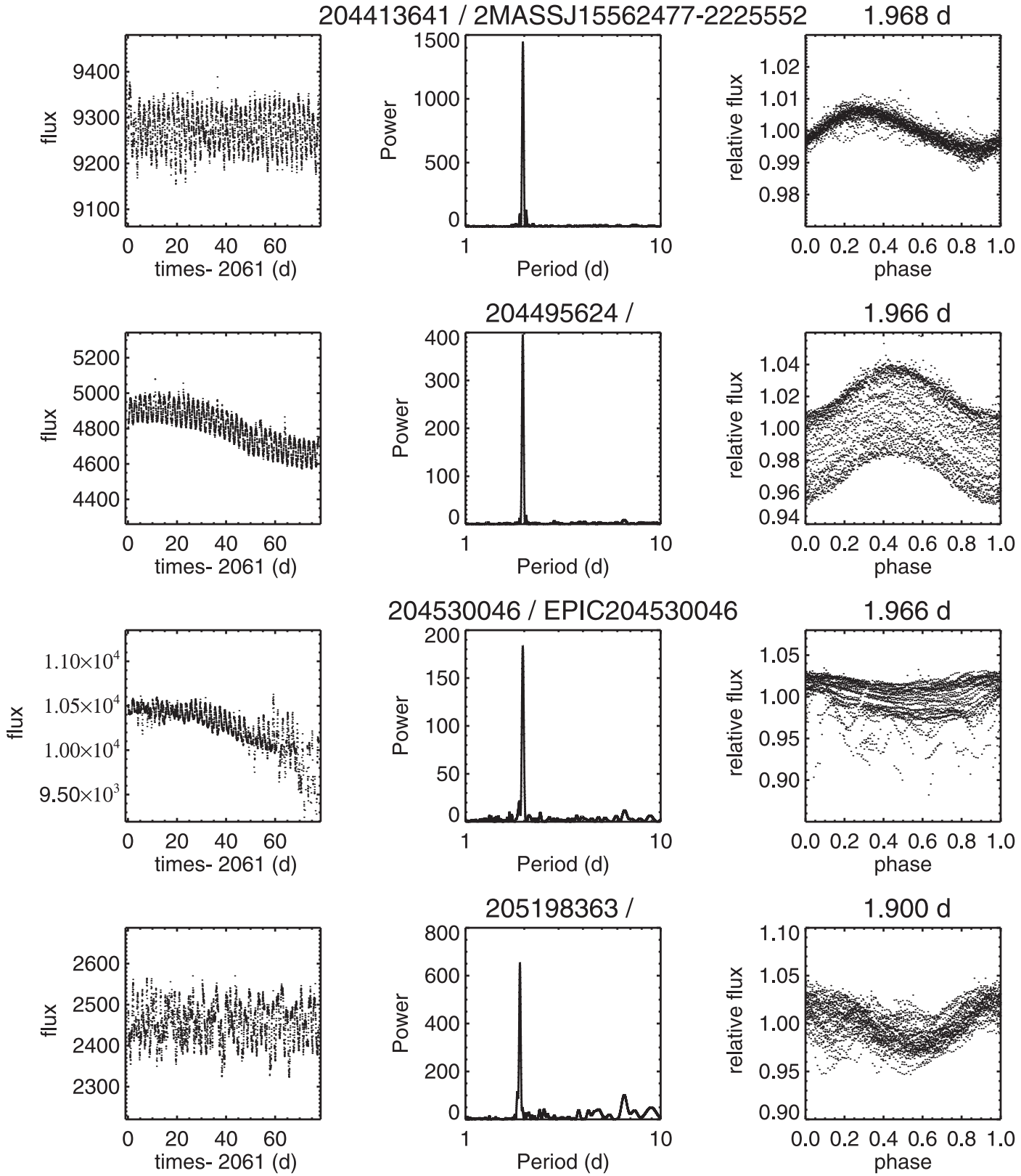

Figure 20. Four examples of light curves (from disked stars) with intrinsic ∼2-day periods. First column: light curve; second column: power spectrum; third column: phased light curve for the ∼2-day period peak in the periodogram. We retained LCs with this kind of behavior as likely real. Specific stars are EPIC 204413641/2MASSJ15562477–2225552 (note that this star also appears in campaign 15, with the same period), EPIC 204495624, EPIC 204530046 (a dipper), and EPIC 205198363.

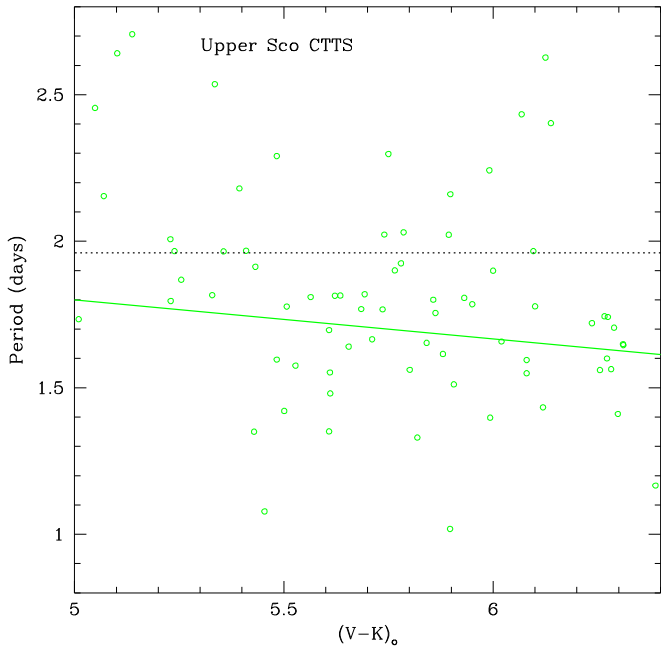

Figure 21. Plot of the periods for the Sco CTTs with $M < 0.32\,M_{\odot}$ versus $V - K$. The solid green line is the linear fit to these data; the dashed black line corresponds to the 1.96-day cadence for the standard *K2* angular momentum dumps. The typical accuracy with which the periods are determined is similar to or smaller than the size of the data points. See text for discussion.

Appendix C
How Complete Is Our Identification of dM Binaries with *K2*?

Two items of information provided in Section 3.1 seem to be in conflict. The first is our statement that we detect periods for about ∼90% of the low-mass members in these young star regions. The second item derives from examination of the CMDs for the Pleiades and Praesepe in the lower half of Figure 2. Those CMDs were meant to highlight that the *K2* dM stars with two periods are, with only a few exceptions, well displaced above the single-star locus, therefore confirming that they are also photometric binaries. What also appears to be true based on those two plots, however, is that an approximately equal number of low-mass photometric binaries (stars displaced more than 0.4 mag above the single-star locus) in these two clusters have only one detected period. Why do we not detect a second period in these stars? Does this issue significantly affect any of our conclusions in the main text concerning the rotation rates of single and *K2*-detected binary stars? We address these issues here.

There are several potential explanations for why there are so many dM stars that appear to be photometric binaries but which have only one period detected with *K2*:

1. There is nonmember contamination.
2. Our census of the *K2* light curve data was incomplete: we failed to identify some of the stars with two real periods.
3. There are single stars masquerading as photometric binaries due to bad photometric data.
4. There are binary members with unusually little photometric variability.
5. There are secondary stars that are too faint to detect their variability with *K2*, but still bright enough to cause a $\Delta V > 0.4$ mag displacement above the single-star locus in the V versus $(V - K_s)_0$ CMD.

We discuss each of these potential explanations in order. We only discuss the Pleiades because it is younger and closer, both of which enhance our ability to quantitatively test how these mechanisms may affect our ability to identify a complete set of M dwarf binaries with *K2*.

C.1. Nonmember Contamination

A foreground nonmember of the cluster could be located above the single-star locus in the cluster CMD even if it is, in fact, a single star. Such a star could be categorized as a photometric binary if plotted in the Pleiades CMD but as a *K2* single assuming it did have a detectable period. Fortunately, *Gaia* DR2 has recently provided us with accurate parallaxes and proper motions for the great majority of the Pleiades *K2* stars, thus allowing us to better ascertain membership status. Figure 22(a) shows a histogram of the *Gaia* DR2 parallaxes for the Pleiades M dwarfs in Figure 2; Figure 22(b) provides the corresponding vector point diagram for those same stars. The stars with discrepant parallaxes in Figure 22(a) are highlighted in Figure 22(b) by red circles. In most cases, the two measures agree; that is, stars with discrepant parallaxes usually also have discrepant proper motions. The number of possible nonmembers flagged in this way is relatively small, amounting to only about 2% of the stars. More importantly, only three of these stars fall significantly above the single-star locus in Figure 2, one of which we have identified as a *K2* binary and the other two as *K2* singles. Therefore, nonmember stars do not significantly contaminate the dM photometric binary census in the Pleiades.

C.2. Previously Missed K2 *Binaries*

We were careful to try to identify all stars with more than one real period in our original *K2* Pleiades paper (Rebull et al. 2016a). However, with more than a thousand stars and half a dozen light curve versions, there is inevitably room for improvement. Also, additional light curve versions have become available, and our own experience in sifting through the data has evolved with time. Therefore, after we had written the initial draft of this paper and identified the correlation between binarity and rotation, we reexamined the light curve data for all of the $M < 0.32\,M_{\odot}$ *K2* stars in the Pleiades. We attempted both to identify new *K2* binaries and to determine if any of our previously identified *K2* binaries should in fact have been assigned only one period. While we did identify a few stars in both categories, the total number of changes was quite modest, and the new plots and statistical measures (which are given in the main text) do not differ significantly from our original results. The changes to the single and *K2* binary categorizations compared to Rebull et al. (2016a) are summarized in Table 7. While some future reprocessing of the *K2* data may yield new results, we are confident that, with the existing *K2* light curves and analysis techniques, our current census of single and binary dMs is as good as we can produce.

C.3. Photometric Uncertainties That Impair Identification of Photometric Binaries

The $(V - K_s)_0$ colors we have used for the low-mass Pleiades and Praesepe members are in some cases measured and in some cases inferred from other photometric systems. For every star, the optical and IR photometry were obtained nonsimultaneously,

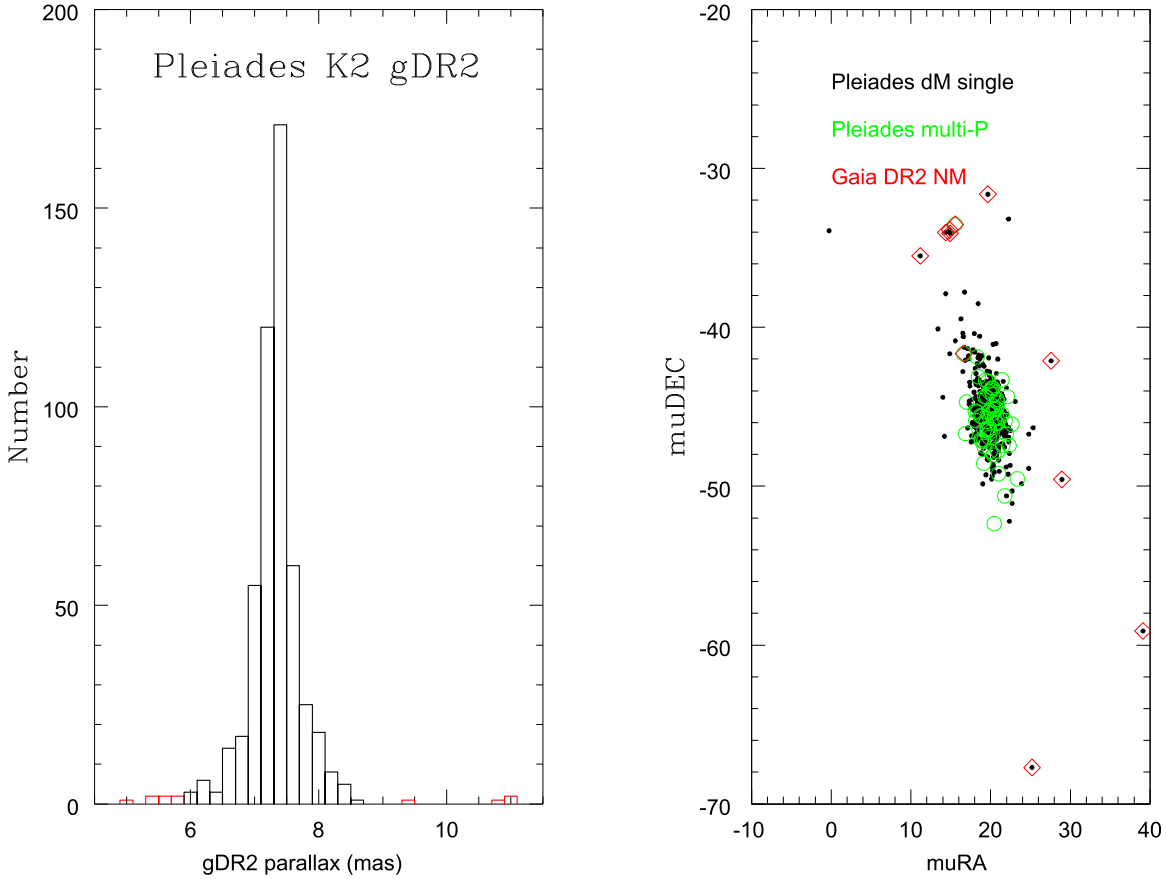

Figure 22. Left: histogram of *Gaia* DR2 parallaxes for candidate $M < 0.32\,M_{\odot}$ Pleiades members from Rebull et al. (2016a). Boxes shown in red are stars we consider probable nonmembers based on their DR2 parallaxes. Right: vector point diagram for candidate $M < 0.32\,M_{\odot}$ Pleiades members from Rebull et al. (2016a) based on *Gaia* DR2 proper motions. *K2* single stars are shown as black dots, *K2* binary stars are shown as green open circles, and stars with discrepant DR2 parallaxes are shown as red diamonds.

Table 7
Changes to Pleiades Rotation Period Relative to Rebull et al. (2016a)

EPIC Number	$(V-K)_o$	P_1 (days)	P_2 (days)	Comments
211040347	6.11	0.3337	0.3650	added P2
211111473	5.90	0.2628	0.2460	added P2
211125179	5.59	0.3484	0.3393	added P2
211030074	5.89	0.1295	0.1367	added P2
210860152	5.49	0.6300	0.6405	added P2
211079163	5.68	0.2350	0.1442	added P2
211103322	5.56	0.3863	⋯	orig P2 that of companion star
211088777	5.77	1.5972	⋯	deleted P2
210940129	6.07	0.7270	⋯	deleted P2

so the photometric variability of these young, spotted stars may in some cases yield estimated colors that differ significantly from what would be obtained with simultaneous data. Therefore, it is possible that some of the stars that are apparent photometric binaries may instead be stars with unusually large errors in their estimated $(V-K_s)_0$ colors.

The *Gaia* DR2 data release provides a means of assessing this issue because DR2 provided photometry in three bands: a very broad G band and narrower G_{BP} (blue) and G_{RP} (red) bands. For each star, the data in these bands were obtained simultaneously, and they are from a space environment that allows significantly better photometric precision than is true for ground-based surveys. And, compared to the heterogeneous nature of our $(V-K_s)_0$ colors, these *Gaia* data are quite homogeneous.

Figure 23 shows a *Gaia* DR2 G_{BP} versus $G_{BP}-G_{RP}$ CMD for the Pleiades dM stars from Figure 2; the *K2* binary stars are shown as red circles. For the bright portion of these stars ($G_{BP} < 17.5$, corresponding to $V \lesssim 17.1$), these data suggest that photometric uncertainties in the $(V-K_s)_0$ colors may indeed have led to the appearance of a larger photometric binary population than is in fact the case. That is, a much smaller fraction of the photometric binaries with $G_{BP} < 17.5$ in Figure 23 are *K2* singles as compared to the same set of stars with $V < 17.1$ in the lower left panel of Figure 2.

Fainter than $G_{BP} = 17.5$, the situation is not so clear. The ratio of *K2* binaries to all stars near the upper envelope of the Pleiades locus still seems to be larger than for the same mass range ($V > 17.1$) in the V versus $(V-K_s)_0$ diagram, but there is also a large population of stars scattered well to the blue of the main locus of Pleiades stars, and the single-star locus seems to broaden considerably for $G_{BP} > 17.5$. We believe the increased scatter in the Pleiades photometry for $G_{BP} > 17.5$ arises from a combination of the faintness of these stars and from known current issues with the DR2 ($G_{BP}-G_{RP}$) colors thought possibly to arise from problems with sky subtraction in regions where there are bright stars or complex backgrounds. Given these issues, it is not possible to draw any conclusions for the $M < 0.32\,M_{\odot}$ mass range concerning the photometric

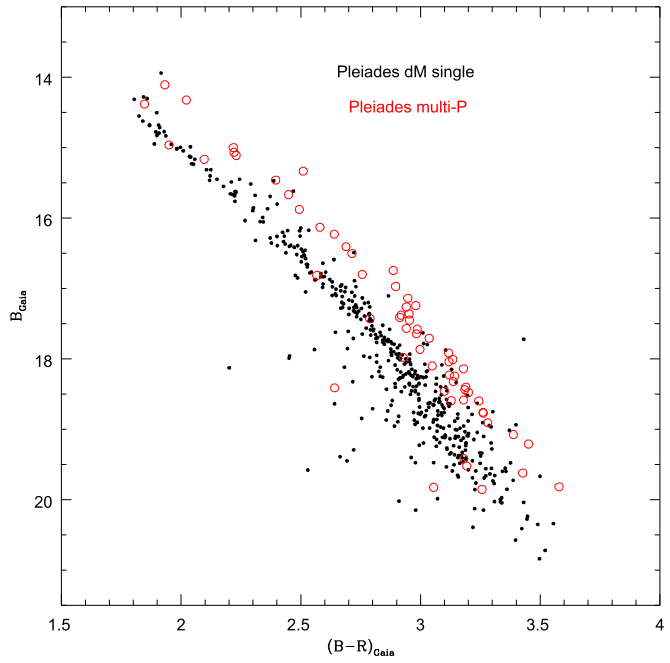

Figure 23. *Gaia* DR2 G_{BP} versus $G_{BP} - G_{RP}$ CMD for the Pleiades dM stars from Figure 2. Black dots are stars with only a single period identified in its *K2* light curve; red open circles are stars identified with two periods from the *K2* data.

binaries that are *K2* singles. However, based on what is seen for $G_{BP} < 17.5$, we believe it is likely that the actual number of photometric binaries that are not detected as *K2* binaries will be significantly lower once we do have better photometry.

C.4. A Population of Photometrically Stable Secondaries?

If viewed from near the rotational pole, even a very nonaxisymmetrically spotted star will show very little photometric variability. This presumably provides a partial explanation for why we do not detect any rotation period for a small fraction (<10%) of the late-type Pleiades candidate members for which we have *K2* data. If the rotational axes of stars in binaries are not perfectly aligned, then binaries would have two chances of near polar alignment to our line of sight. However, while this might contribute to the presence of some *K2* single stars among the photometric binaries, it could not explain the very large number shown in the lower left panel of Figure 2.

A potentially more serious problem could occur if photometric variability amplitude and rotation period were strongly linked for young stars, in the sense of lower amplitudes for slower rotators. In that case, the *K2* singles that are photometric binaries could be systems with one component that is unusually slowly rotating and hence has little periodic signature in its *K2* light curve. If this explanation were valid, it could make our finding of faster rotation in binaries relative to singles be a selection effect, in that our sample is missing the most slowly rotating binary star members.

To test this hypothesis, we have carefully remeasured the photometric amplitudes of all the $M < 0.32\,M_{\odot}$ Pleiades dM stars for which we detect only one period. We plot these amplitudes versus both period and $(V - K_s)_0$ color in Figure 24. Those plots mostly show that there is a wide spread in photometric amplitude at a given period and at a given color. The range in amplitude by far exceeds any possible correlation between amplitude and period or amplitude and color. One thing that is evident (right panel of Figure 24) is that for the faintest/reddest stars, we probably are only detecting the largest-amplitude variables, a likely occurrence since these stars are near the faint limit for identifying periods with *K2*.

Figure 24 thus provides no basis for there being a hidden population of slowly rotating, low-amplitude companions that our *K2* data would have failed to detect.

C.5. Secondaries Too Faint for K2 *to Detect Periods*

K2 can detect rotation periods in remarkably faint stars. The faintest (lowest mass) star for which we report a detected period in the Pleiades has $V \sim 20.5$, or *K2* mag ~17.3. It is likely that we only detect periods for the most photometrically variable stars near this limiting magnitude, as suggested by Figure 24(b). The limiting magnitude to which we can detect periods also might be affected by whether the star is in a binary or not, since the light from the other star in the system will act as an additional noise source. Since the single-star bright end of our mass range in the Pleiades ($0.32\,M_{sun}$) has a *V* magnitude only ~2.5 mag brighter than the limiting magnitude for detecting periods, it is plausible that we might fail to detect periods in the secondary components of photometric binaries if the secondary is too faint.

In order to assess this a little more quantitatively, we determined system *V* and $(V - K_s)_0$ magnitudes for hypothetical low-mass Pleiades binaries, using an empirical *V* versus $(V - K_s)_0$ single-star locus analogous to that shown in Figure 14. The primary in all cases had $V = 18.0$ and $(V - K_s)_0 = 5.4$. Secondaries ranged down to $V = 20.25$, the faint limit for our single-star locus. For an equal-brightness system, the combined light of the binary is shifted 0.75 mag above the single-star locus, as expected. However, even for the faintest secondary, the predicted shift above the single-star locus is ~0.6 mag. Thus, it is entirely possible for many of the photometric binaries among the $M < 0.32\,M_{\odot}$ Pleiades stars to have secondaries that are simply too faint to detect periods with *K2*.

C.6. Conclusions Concerning Our K2 *Binary Sample*

The *V* versus $(V - K_s)_0$ CMD for the Pleiades and Praesepe M dwarfs (Figure 2, lower panels) appeared to show a large population of photometric binaries for which we only detected one period with *K2*. In this appendix, we have attempted to determine the cause for this apparent anomaly. Based on our analysis, three of the potential explanations we have examined do not, in our opinion, significantly help to explain this anomaly: (1) nonmember contamination, (2) incomplete or inaccurate identification of multiple periods in our *K2* sample, and (3) failure to detect a hypothetical population of very slowly rotating companion stars due to their postulated low amplitudes of photometric variability. Instead, we believe our analysis has demonstrated that there are two primary or likely explanations for the apparent excess of stars displaced well above the single-star locus in Figure 2 but having only one *K2* period. First, we believe that errors in the $(V - K_s)_0$ colors have inflated the number of apparent photometric binaries among the Pleiades dM stars, and that with better photometry these stars often will fall within the single-star locus. Second, particularly for the lowest mass stars, if there is a range of secondary to primary star mass ratios, many of the binary systems will be displaced well above the single-star locus but have secondaries

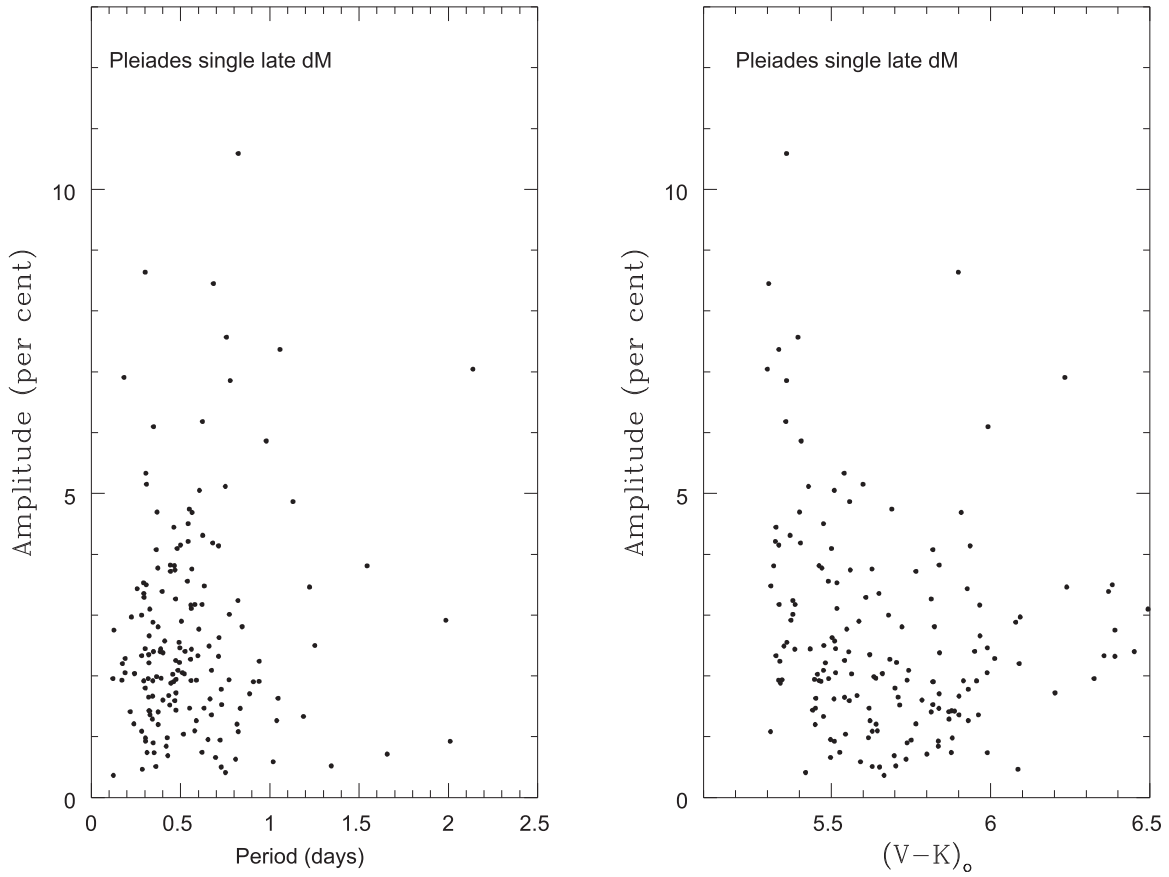

Figure 24. Left: full amplitude of the phased *K2* light curves of the single, late-type Pleiades dM stars versus our derived periods. Right: the same photometric amplitudes but now plotted versus the $(V - K_s)_0$ color of the star. Both plots primarily show a large scatter at any given period or $(V - K_s)_0$ color, with no significant correlation between amplitude and period or color.

that are too faint for *K2* to detect their periods. Based on this analysis, the apparent excess of photometric binaries that are *K2* singles is unlikely to affect any of our conclusions with respect to the rotation rates of single versus binary young, low-mass stars.

ORCID iDs

John Stauffer https://orcid.org/0000-0003-3595-7382
Luisa M. Rebull https://orcid.org/0000-0001-6381-515X
Ann Marie Cody https://orcid.org/0000-0002-3656-6706
Marc Pinsonneault https://orcid.org/0000-0002-7549-7766
David Barrado https://orcid.org/0000-0002-5971-9242
Jerome Bouvier https://orcid.org/0000-0002-7450-6712
Trevor David https://orcid.org/0000-0001-6534-6246

References

Affer, L., Micela, G., Favata, F., et al. 2013, MNRAS, 430, 1433
Aigrain, S., Llama, J., Ceillier, T., et al. 2015, MNRAS, 450, 3211
An, D., Terndrup, D., Pinsonneault, M., et al. 2007, ApJ, 655, 233
Ansdell, M., Gaidos, E., Rappaport, S., et al. 2016, ApJ, 816, 69
Azulay, R., Guirado, J., Mercaide, J., et al. 2017, A&A, 607, A10
Bergfors, C., Brandner, W., Janson, M., et al. 2010, A&A, 520, 54
Boesgaard, A., & Budge 1988, ApJ, 332, 410
Bouvier, J., Bertout, C., Benz, W., & Mayor, M. 1986, A&A, 165, 110
Bouvier, J., Forestini, M., & Allain, S. 1997, A&A, 326, 1023
Browning, M. 2008, ApJ, 676, 1262
Chen, Y., Girardi, L., Bressan, A., et al. 2014, MNRAS, 444, 2525
Close, L., Thatte, N., Nielson, E., et al. 2007, ApJ, 665, 736
Cummings, J., Deliyannis, C., Maderak, R., & Steinhauer, A. 2017, AJ, 153, 128
David, T., Conroy, K., Hillenbrand, L., et al. 2016, AJ, 151, 112
Douglas, S., Agueros, M., Covey, K., et al. 2016, ApJ, 822, 47
Douglas, S., Agueros, M., Covey, K., & Kraus, A. 2017, ApJ, 842, 83
Duchene, G., & Kraus, A. 2013, ARAA, 51, 269
Duquennoy, A., & Mayor, M. 1991, A&A, 248, 485
Fischer, D., & Marcy, G. 1992, ApJ, 396, 178
Gaia Collaboration, Prusti, T., de Bruijne, J. H. J., et al. 2016, arXiv:1609.04172
Gallet, F., & Bouvier, J. 2015, A&A, 577, 98
Ghez, A., Neugebauer, G., & Matthews, K. 1993, AJ, 106, 2005
Ghosh, P., & Lamb, F. 1979, ApJ, 234, 296
Gillen, E., Hillenbrand, L., David, T., et al. 2017, ApJ, 849, 11
Harris, R., Andrews, S., Wilner, D., & Kraus, A. 2012, ApJ, 751, 115
Hartmann, L., Hewett, R., Stahler, S., & Mathieu, R. 1986, ApJ, 309, 275
Herbst, W., Ba0ler-Jones, C., & Mundt, R. 2001, ApJL, 554, L197
Howell, S., Sobeck, C., Haas, M., et al. 2014, PASP, 126, 398
Janson, M., Hormuth, F., Bergfors, C., et al. 2012, ApJ, 754, 44
Königl, A. 1991, ApJL, 370, L39
Kraus, A., Cody, A., Covey, K., et al. 2015, ApJ, 807, 3
Kraus, A., Douglas, S., Mann, A., et al. 2017, ApJ, 845, 72
Kraus, A., Ireland, M., Huber, D., et al. 2016, AJ, 152, 8
Kraus, A., Ireland, M., Martinache, F., & Lloyd, J. 2008, ApJ, 679, 762
Kuker, M., & Rudiger, G. 1997, A&A, 328, 253
Lafreniere, D., Jayawardhana, R., van Kerkwijk, M., et al. 2014, ApJ, 785, 47
Luhman, K., Stauffer, J., & Mamajek, E. 2005, ApJL, 628, L29
Mann, A., Feiden, G., Gaidos, E., et al. 2015, ApJ, 804, 64
Meibom, S., Mathieu, R., & Stassun, K. 2007, ApJL, 655, L155
Moraux, E., Artemko, S., Bouvier, J., et al. 2013, A&A, 560, 13
Morin, J., Donati, J.-F., Petit, P., et al. 2010, MNRAS, 407, 2260
Pace, G., Pasquini, L., & Francois, P. 2008, A&A, 489, 403
Pinsonneault, M., Kawaler, S., & Demarque, P. 1990, ApJS, 74, 501
Radick, R., Thompson, D., Lockwood, et al. 1987, ApJ, 321, 459
Rappaport, S., Swift, J., Levine, A., et al. 2014, ApJ, 788, 114

Rebull, L., Stauffer, J., Bouvier, J., et al. 2016a, AJ, 152, 113
Rebull, L., Stauffer, J., Bouvier, J., et al. 2016b, AJ, 152, 114
Rebull, L., Stauffer, J., Cody, A., et al. 2018, arXiv:1803.04440
Rebull, L., Stauffer, J., Hillenbrand, L., et al. 2017, ApJ, 839, 92
Rebull, L., Wolff, S., Strom, S., & Makidon, R. 2002, AJ, 124, 546
Reid, I. N., & Gizis, J. 1997, AJ, 113, 2246
Reinhold, T., Reiners, A., & Basri, G. 2013, A&A, 560, 4
Santos, A., Cunha, M., Avelino, P., et al. 2017, A&A, 599, 1
Shan, Y., Yee, J., Bowler, B., et al. 2017, ApJ, 846, 93
Sills, A., Pinsonneault, M., & Terndrup, D. 2000, ApJ, 534, 335
Skrutskie, M., Cutri, R. M., Stiening, R., et al. 2006, AJ, 131, 1163
Skumanich, A. 1972, ApJ, 171, 565
Stauffer, J., Rebull, L., Bouvier, J., et al. 2016, AJ, 152, 115
van Cleve, J. E., Howell, S. B., Smith, J. C., et al. 2016, PASP, 128, 075002
Werner, M., Roellig, T., Low, F., et al. 2004, ApJS, 154, 1
White, T., Pope, B., Antoci, V., et al. 2017, MNRAS, 471, 2882
Wright, E., Eisenhardt, P. R. M., Mainzer, A. K., et al. 2010, AJ, 140, 1868
Zwintz, K., Fossati, L., Ryabchikova, T., et al. 2014, Sci, 345, 550